~~CONFIDENTIAL~~ UNCLASSIFIED

ANL-5566
Reactors - Special Features
of Military Package Power
Reactors
M-3679 (18th edition)
This document consists of 62 pages
No. 76 of 100 copies Series B

ARGONNE NATIONAL LABORATORY
P. O. Box 299
Lemont, Illinois

ALPR PRELIMINARY DESIGN STUDY
(ARGONNE LOW POWER REACTOR)
PHASE I

by

M. Treshow, Project Engineer
E. Hamer
H. Pearlman
D. Rossin
D. Shaftman

Reactor Engineering Division

CLASSIFICATION CANCELLED
DATE 6-9-58
For The Atomic Energy Commission
Chief, Declassification Branch

April 20 1956

Operated by The University of Chicago
under
Contract W-31-109-eng-38

~~CONFIDENTIAL~~ UNCLASSIFIED

DISCLAIMER

ANL-5566
Reactors - Special Features of Military Package Power Reactors

Distribution	Copy No.
Argonne National Laboratory	1
AF Plant Representative, Burbank	2
AF Plant Representative, Marietta	3
Albuquerque Operations Office	4
Alco Products, Inc.	5
Armed Forces Special Weapons Project, Sandia	6
Armed Forces Special Weapons Project, Washington	7
Army Chemical Center	8
Atomic Energy Commission, Washington	9-12
Battelle Memorial Institute	13
Bettis Plant (WAPD)	14-15
Bureau of Medicine and Surgery	16
Bureau of Ships	17
Bureau of Yards and Docks	18
Chicago Operations Office	19-20
Chicago Patent Group	21
Chief of Naval Research	22
Combustion Engineering, Inc. (CERD)	23
Continental Army Command	24
duPont Company, Aiken	25
duPont Company, Wilmington	26
Engineer Research and Development Laboratories	27
General Electric Company (ANPD)	28-29
General Electric Company, Richland	30-35
Hartford Area Office	36
Headquarters, Air Force Special Weapons Center	37
Iowa State College	38
Knolls Atomic Power Laboratory	39-41
Los Alamos Scientific Laboratory	42-43
National Advisory Committee for Aeronautics, Cleveland	44
National Advisory Committee for Aeronautics, Washington	45
Naval Research Laboratory	46-47
New York Operations Office	48
North American Aviation, Inc.	49
Nuclear Development Corporation of America	50
Office of the Chief of Naval Operations (OP-361)	51
Patent Branch, Washington	52
Phillips Petroleum Company (NRTS)	53-55
Pratt and Whitney Aircraft Division (Fox Project)	56
Sandia Corporation	57
School of Aviation Medicine	58
Sylvania Electric Products, Inc.	59
The Surgeon General	60
Union Carbide Nuclear Company (ORNL)	61-64
USAF Headquarters	65
USAF Project RAND	66
U. S. Naval Postgraduate School	67
U. S. Naval Radiological Defense Laboratory	68
University of California Radiation Laboratory, Berkeley	69
University of California Radiation Laboratory, Livermore	70
Wright Air Development Center (WCOSI-3)	71-75
Technical Information Service Extension, Oak Ridge	76-100
Total	100

TABLE OF CONTENTS

TABLE OF CONTENTS

LIST OF TABLES

LIST OF FIGURES

ALPR PRELIMINARY DESIGN STUDY
(ARGONNE LOW POWER REACTOR)
PHASE I

by
M. Treshow, Project Engineer,
E. Hamer, H. Pearlman
D. Rossin, D. Shaftman

ABSTRACT

A preliminary design study, Phase I of the ALPR project, has been made in accordance with the Army Reactors Branch specifications for a nuclear "package" power plant with a 200-260-kw electric and 400 kw heating capacity. The plant is to be installed at the Idaho Reactor Testing Station as a prototype for remote arctic installations.

The "conventional" power plant as well as the exterior reactor components are described in the accompanying report and cost estimate by Pioneer Service and Engineering Company, Architect-Engineers for the project.

"Nuclear" components of the reactor are designed by Argonne National Laboratory as described in the present report. (auth)

I. INTRODUCTION AND GENERAL SPECIFICATIONS

Reference is made to M. Treshow, et al., "Design Study of a Nuclear Power Plant for 100-kw Electric and 400-kw Heat Capacity," ANL-5452 (May 1955), which is a study of a smaller power plant designed for similar conditions.

The present ALPR study is based on a greater power demand, essentially according to specifications issued October 7, 1955 with minor deviations mutually agreed upon later. Also the original requirement for "unmanned" operation has been modified.

The building structure has been modified so as to allow reloading of fuel in the reactor at any time of the year.

The essential specifications of the plant are summarized below:

Capacity: 200-kw electrical load which may be increased to 260 kw provided the ambient temperature is not higher than 40F. In addition, a maximum heating load equal to 400 kw.

Frequency: 60 cps with a tolerance of ± 1/2 cps.

Voltage: 120/208 volts, 3 phase, 4 wire with a tolerance of ± 5%.

Power Factor: 0.8 assumed.

Standby Equipment: Diesel electric plant at full capacity.

Transportability: Airlift.

Site Materials for Construction: Gravel and water.

Ambient Temperatures: -60F to + 60F.

Wind Velocity: Maximum of 125 mph.

Building Site: Permafrost.

Maximum Building Height: 50 ft above ground level.

Control: The system is to be "demand controlled" within a range from 20-kw net load to the maximum demand of 260 kw. In this range the load may change gradually or it may change intermittently in steps as big as 60 kw at a time. A total of 25 seconds is allowed between steps of this magnitude. The plant must return to stable operation (frequency error less than 1/2 cps) in less than 5 sec after each load change. In order to meet this requirement it is permissible to maintain a normal steam bypass equal to the difference in steam demand before and after a 60-kw load change. The bypassed steam is to be available for the space heating system.

Control of all equipment is to be carried out from one control and instrument panel.

Core Life: A core life of 3 yr operated with a plant factor of 0.7 will be attempted. This is considered the maximum life expectancy. In case of the prototype reactor, nickel-aluminum alloy will be tried for the reactor core due to the low cost and the promising results from corrosion tests carried out at Argonne in boiling autoclaves and in-pile radiation loops.

Personnel: The station will be operated for prolonged periods of time with a minimum of expert supervision. The personnel will primarily be trained in electronics with a minimum of reactor technology.

II. REACTOR GENERAL DESCRIPTION AND DESIGN DATA

A. General Description (Figs. 1 and 2)

The reactor is a boiling reactor comparable to "BORAX III" which has been operated for some time by Argonne National Laboratory at the Idaho Testing Station.

The two significant changes are that the ALPR must be equipped with an automatic control system tied to a variable power demand and that it must be able to remain in continuous operation for several years without refueling and with a minimum of attendance and maintenance.

Other special features of the ALPR reactor are the following:

1. The fuel plates will be made of nickel-aluminum alloy enriched with U^{235} and will contain an amount of burnable poison (boron) designed to secure a long-term operating period without a prohibitive change in reactivity.

2. Refueling can take place without removing the pressure vessel cover. This operation is carried out through nine control rod thimbles.

3. The core is built with space for additional fuel assemblies and additional control rods to make it possible to test the prototype reactor for greater power levels than required by the present ALPR specifications.

4. The reactor is equipped with dual feedwater inlets so that power can, within certain limits, be regulated by a variable degree of feedwater preheating.

5. The reactor biological shield is made inexpensively of local gravel thereby avoiding considerable thermal stresses which would occur in a cold climate in a solid concrete shield heated from the inside.

B. Design Data

1. Performance

Maximum operating power level, mw	3.0
Steam pressure, psia	300
Steam temperature, degrees F	417
Normal feedwater temperature, degrees F	133
Maximum operating steam production, lb/hr	8,500

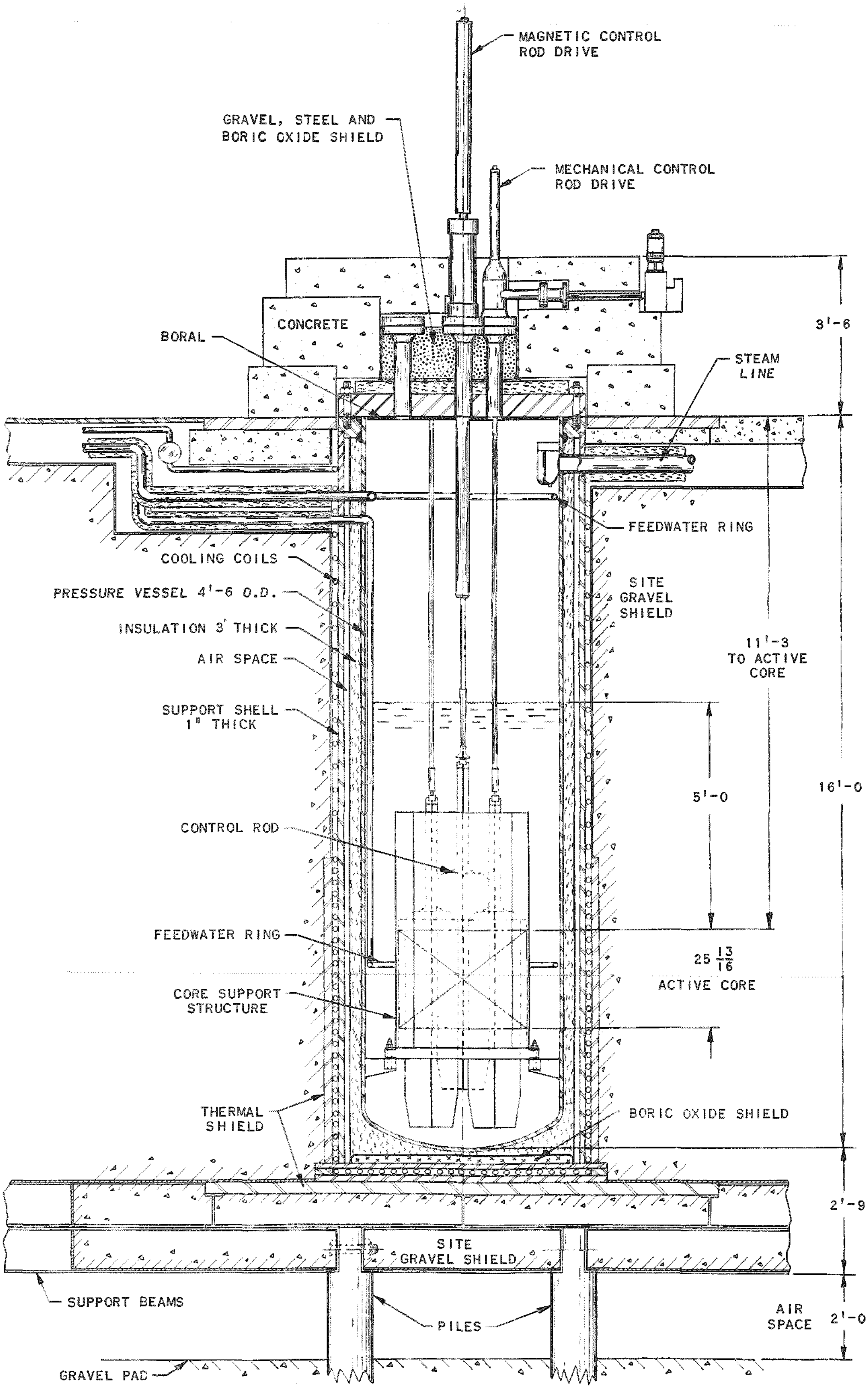

FIG. 1
REACTOR VERTICAL SECTION

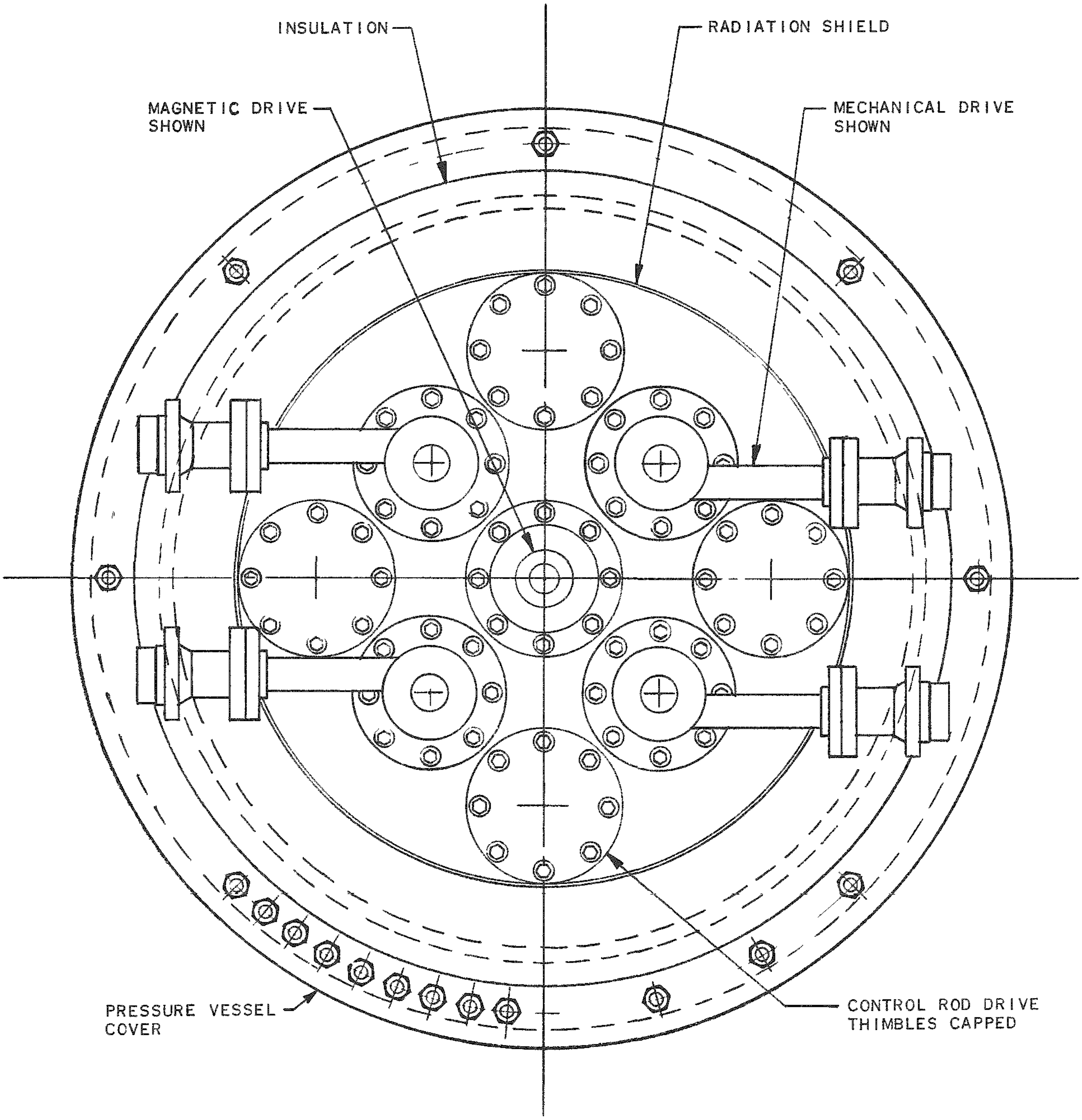

FIG. 2
REACTOR TOP VIEW

2. Core

Length of active core, in.	25.8
Horizontal cross section, in.	
Minimum, approximately	28 x 28
Maximum, approximately	33 x 33

3. Fuel Assemblies (BORAX Type with Aluminum-Nickel Alloy)

Geometry, in.	3-7/8 x 3-7/8
No. of elements, minimum loading	40
No. of elements, maximum loading	60
Total thickness of fuel plates (0.040-inch meat, 0.030-inch clad), in.	0.100
Average water channel gap, in.	0.287
Core heat transfer area (minimum loading), sq ft	540
Fuel in 40 assemblies, kg U^{235} (approx.)	13
Average heat flux at maximum power level and minimum loading, Btu/(hr) (sq ft)	20,800

4. Control Rods

Composition: cadmium, clad with aluminum-nickel alloy

Geometry

At minimum loadings: 5 cross rods @ 14 in. x 14 in., 1/4 in. thick.

At maximum loading: 4 T-rods @ 7 in. x 12 in. added.

5. Pressure Vessel

Outside diameter, ft	4-1/2
Total height, ft	16
Level of water above core, ft	5
Average volume of "steam dome," cu ft	90
Average content of water in pressure vessel, lb	6,000

III. REACTOR COMPONENTS

A. Reactor Core

General views of the ALPR core are shown in Figs. 1, 3, and 4. With the exception of certain minor items, such as fuel element spacer springs that are of stainless steel, the entire core is fabricated of an alloy of type 2S aluminum and nickel, called aluminum-nickel. The control rod cladding and the fuel element cladding and end pieces are also of this alloy, whose nominal composition is given in Table 1.

Table 1

NOMINAL COMPOSITION OF ALUMINUM-NICKEL

	Wt %
Aluminum	98.5
Iron	0.3
Nickel	1.0
Cobalt (assumed = 2% of Ni)	0.02
Balance (silicon, copper, etc.)	0.2

Weights and surface areas of the core and related components are summarized in Table 2.

1. Core Support

The core consists of a frame of cross-welded bars, bolted at eight points to supports that are welded to the side of the pressure vessel. The core support structure - a welded and riveted assembly of the stanchions, control rod shrouds, and fuel element grid - is welded to the lower frame at the bases of the fourteen stanchions. The fuel elements fit into square cross section slots in the grid.

a. Lower Frame

The lower frame is shown in vertical section in Fig. 3 and is dotted in the horizontal section, Fig. 4. It is made of 1/2-inch by 3-inch bars, notched and welded at cross points. Bearing pads are attached at eight locations on the frame perimeter, and these engage lugs that are part of the core supports welded to the side of the pressure vessel.

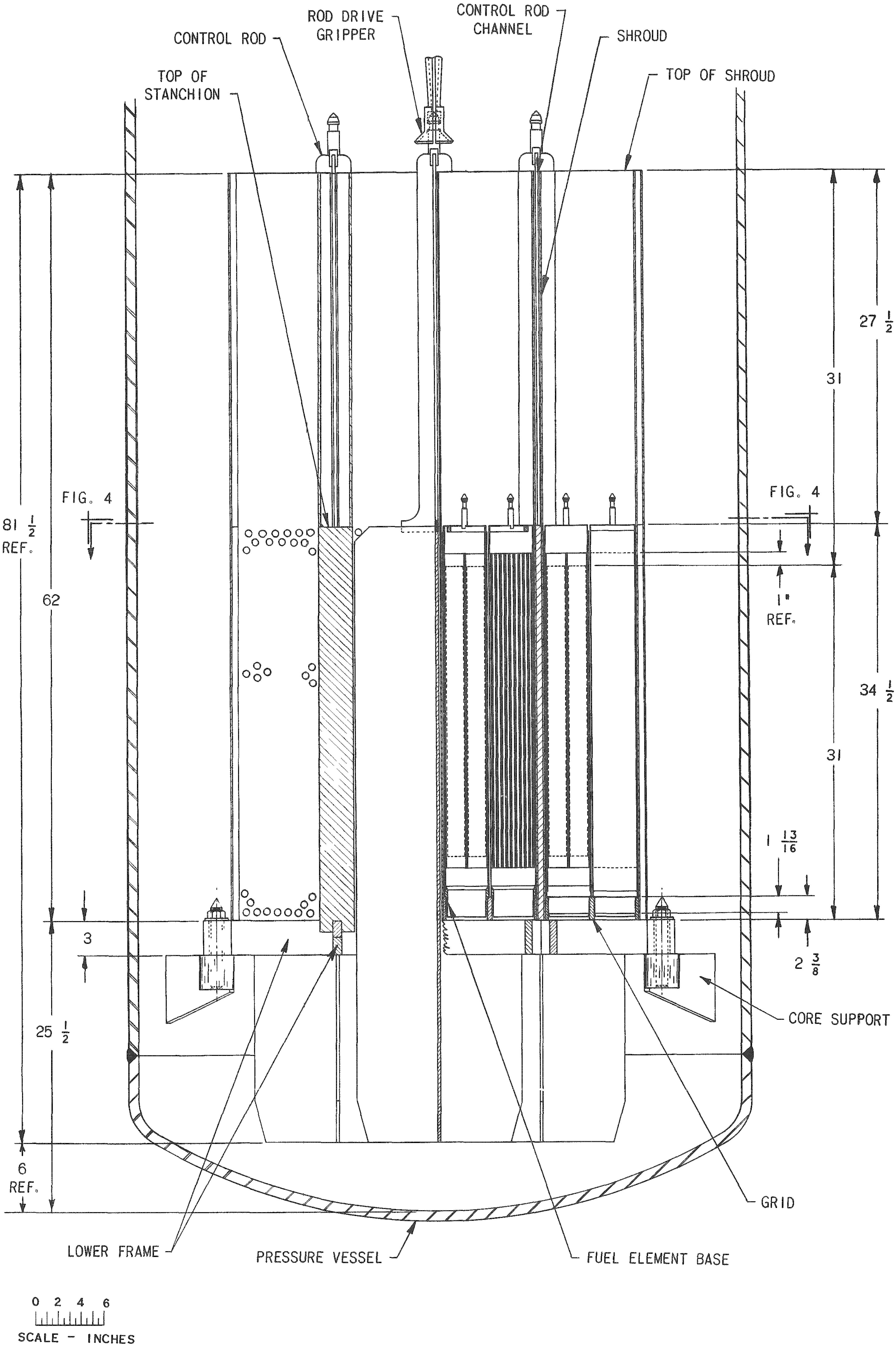

FIG. 3
CORE VERTICAL SECTION

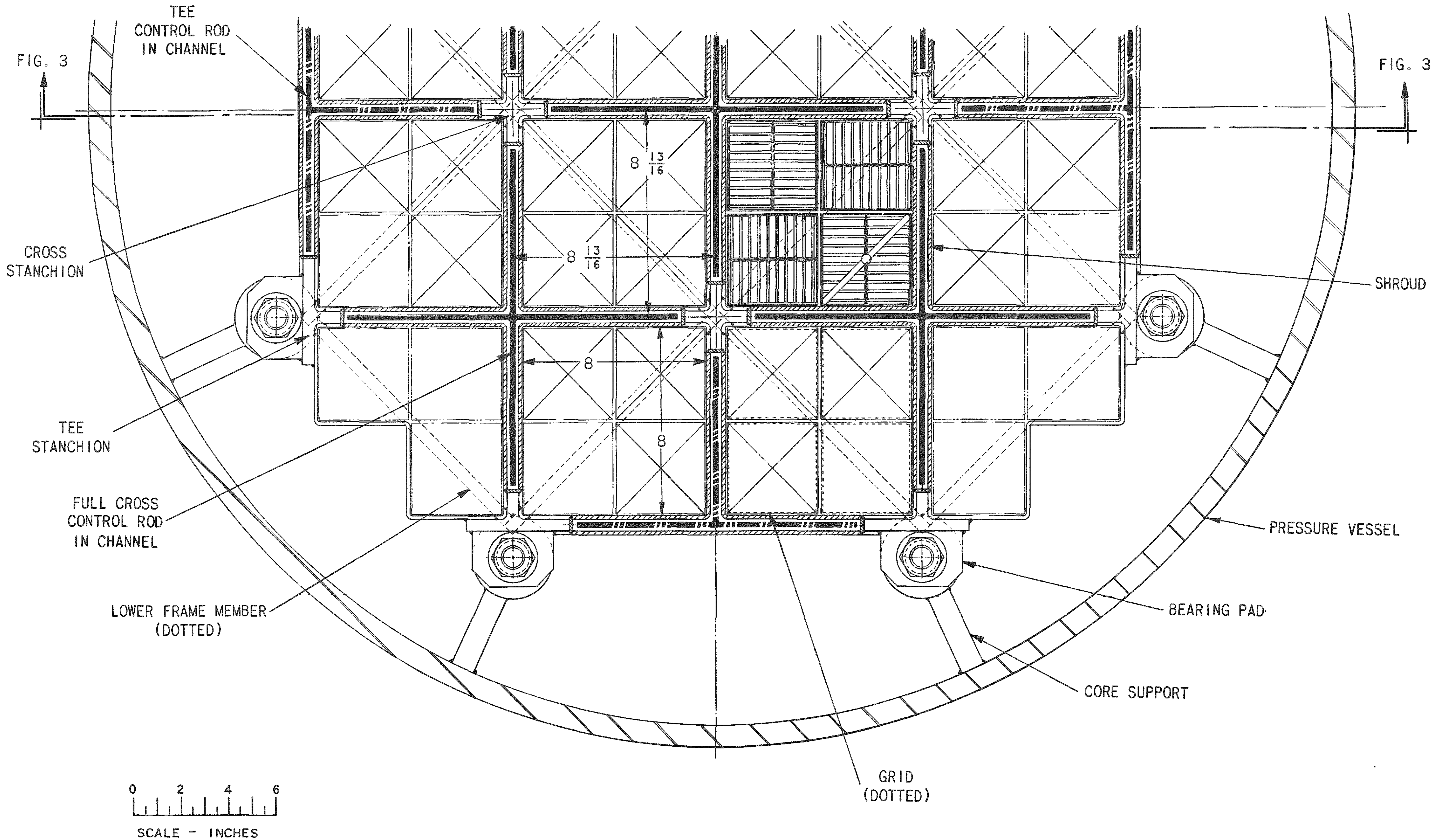

FIG. 4
CORE PLAN SECTION

DECLASSIFIED
DECLASSIFIED

Table 2

CORE COMPONENT WEIGHTS AND AREAS

Item	Weight (lb)	Area (sq ft)	Heat Transfer Area (sq ft)
Reference fuel assembly:			
One assembly	14-3/4	1-3/4	1-1/4
Forty assemblies	590	70	50
Sixty assemblies	885	105	62
Alternate fuel element:			
One assembly	14-1/2	1-1/2	1-1/8
Forty assemblies	580	60	45
Sixty assemblies	870	90	67
Core:			
Lower frame, stanchions, and control rod shrouds	860	39-1/2	
Control rod:			
Four-blade	49	2-3/8	
Three-blade	37	1-3/4	

b. Box Structure

As is indicated in Fig. 4, the core is divided into sixteen boxes. Twelve boxes (each to contain four fuel elements) at the center and sides are of square cross section; the four corner boxes are contoured to contain three fuel elements each. The maximum core capacity is sixty elements. The sides of the boxes serve as shrouds to define the control rod channels. There are five full-cross channels and four tee channels to be used if necessary.

The shroud boxes are made of 5/32-inch thick plate, bent to shape and welded closed. Inside dimensions of the square shroud boxes are 8 in. by 8 in.; the control rod channels defined by the shrouds, are 1/2 in. wide (see Fig. 4). The shrouds are riveted along the length of the stanchions. Total shroud length is 62 in. The lower half is perforated by 1/2-inch diameter holes to equalize water pressure. The upper half is of solid metal to confine the control rods and also to prevent control rod rattling caused by action of the turbulent water above the fuel elements when the rods are withdrawn from the core (see Fig. 3).

To facilitate flow of water from the tops of the fuel elements to the downcomer area at the sides of the pressure vessel the corners of the shroud boxes are slotted along the upper 27-1/2 in. of their length (see Fig. 4). The opening across the slot is about 1-1/2 in. wide. The ends of the control rod channels are closed by welding strips over the upper 27-1/2-inch length across the edges of the slots.

The fuel element bases fit into square slots formed by a grid of bars. The cross bars are 3/8 in. by 2-3/8 in., notched and welded at the cross point. The sides are 3/16-inch by 2-3/8-inch bars, welded to the ends of the cross bars. After it is machined, the grid is fastened into the lower 2-3/8 in. of the 8-inch by 8-inch shroud box by riveting or welding.

Each completed grid consists of four square openings, 3-5/8 in. by 3-5/8 in., enclosed within the 8-inch by 8-inch shroud box. The spacing provides for an 1/8-inch clearance between fuel elements and a 1/16-inch clearance between fuel element and shroud.

To maintain fuel-element spacing, stainless steel springs are fastened at the four sides of the fuel element, near the top.

Inactive fuel elements with solid aluminum-nickel plates will be placed in the core positions not occupied by active fuel elements, in order to complete partially filled shroud boxes.

Figure 7 shows the forty fuel-element core loading for the reference design and the extra fuel-element positions.

2. Fuel Elements

The features of the reference design fuel element, and also of an alternate design, are summarized in Table 3.

a. Reference Design

The reference design chosen for the ALPR fuel element is shown in Fig. 5. It is similar in general outline to the BORAX-III fuel elements.

The fuel plates consist of a 0.040-inch thick center portion ("meat") of enriched uranium-aluminum alloy. This is clad on both sides with aluminum-nickel, 0.030-inch thick. Each fuel element contains twenty plates.

Table 3

SUMMARY OF REFERENCE AND ALTERNATE ALPR FUEL ASSEMBLY DESIGNS[a]

	Reference Design	Alternate Design
Cross Section of Assembly[b]	3.870 x 3.870	3.870 x 3.870
No. of plates/assembly	20	9
Fuel plate dimensions (before assembly)	27.8 x 2.330 x 0.100	27.8 x 3.750 x 0.120
Thickness of water channel	0.287	0.310
"Meat" dimensions	25.8 x 1.555 x 0.040	25.8 x 3.500 x 0.050
Cladding thickness	0.030	0.035
Meat volume/plate	26.3 cm^3	74.11 cm^3
Approx. weight Al in meat/plate	84 gm	200 gm
Weight U^{235}/plate	16.25 gm	36.11 gm
Weight U (93.2% U^{235})/ plate	17.4 gm	38.8 gm
Weight normal B/plate	0.20 gm	0.44 gm
Approx. wt % U in meat	19.7%	16.2%
Approx. wt % B in meat	0.2%	0.2%
Weight U^{235}/assembly	325 gm	325 gm
Weight U/assembly (approx.)	350 gm	350 gm
Weight B/assembly (approx.)	4.0 gm	4.0 gm

Notes: (a) In the reference core design, approximately 13 kg of U^{235} and approximately 30 gm of B^{10} are contained in a total of 40 fuel assemblies. At the present stage of calculations, it appears that the final values will range between 13 and 14 kg of U^{235} and 20 to 30 gm of B^{10}.

(b) Dimensions are in inches, unless otherwise indicated.

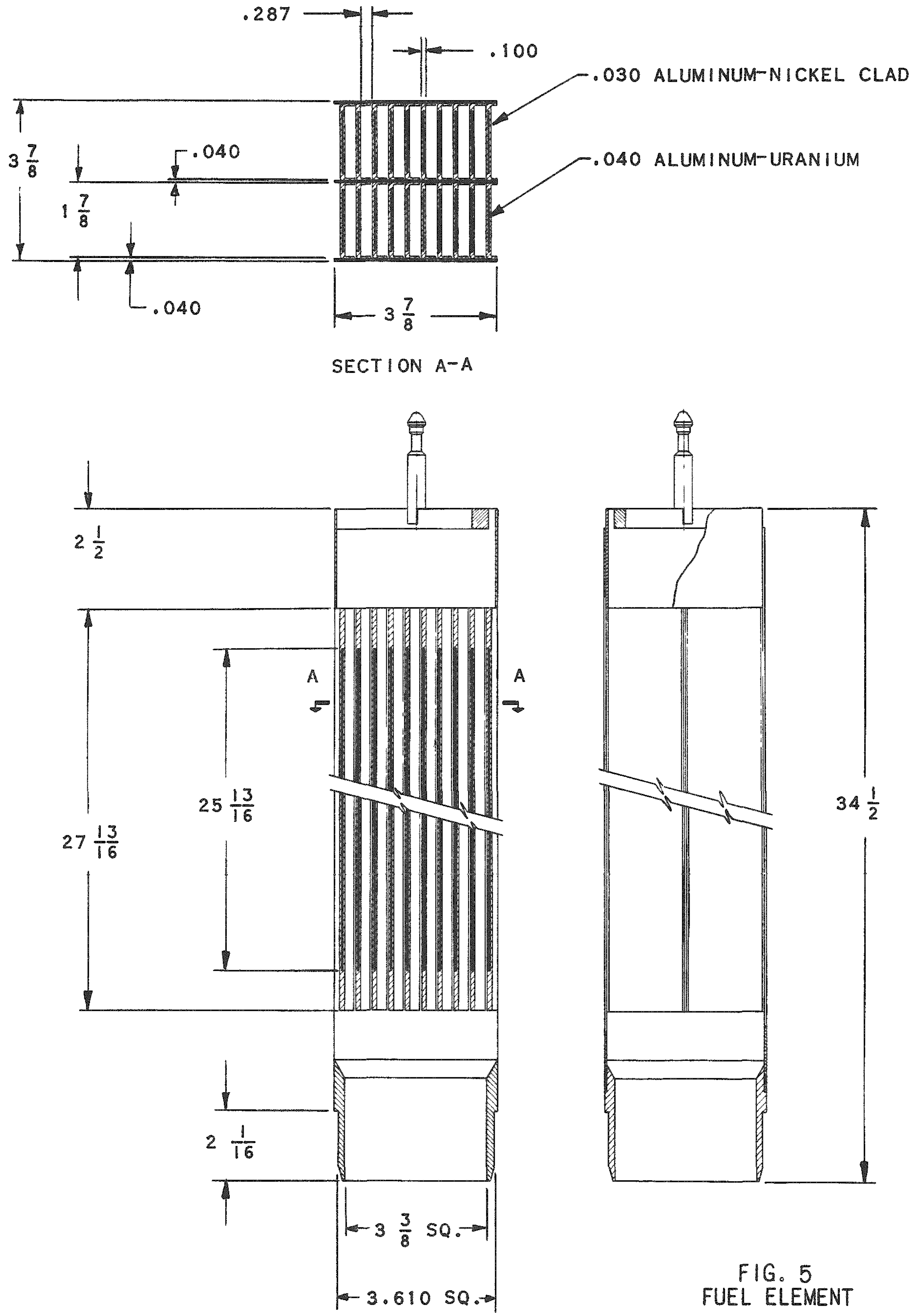

FIG. 5
FUEL ELEMENT

The fuel plates are assembled to 0.040-inch thick side and center plates by spot-welding. The inactive sides of the 0.100-inch thick fuel plates in the ALPR reference design, after bending, are machined down to 0.040-inch thickness.

The fuel element base is machined from a casting. It is fastened to the sides of the fuel plate section by plug welding. The base provides bearing in the grid and is tapered at the bottom to facilitate insertion.

The fuel element top is a box section formed of bent sheet, and is spot-welded to the sides of the fuel plate section. A bar is welded diagonally across the top of the box section. This bar supports the fitting that serves as handle for the complete assembly.

b. Alternate Design

The alternate fuel element design, shown in Fig. 6, consists of 0.120-inch thick plates assembled into 0.125-inch thick side plates by plug-welding. The over-all dimensions of the assembly are identical to the reference design.

The fuel plate consists of a 0.050-inch thick center portion of aluminum-uranium alloy, clad with 0.035-inch thick aluminum-nickel. The "meat" is 3-1/2 in. wide by 25.8 in. long. The finished clad plate width is 3-3/4 in. wide and 27.8 in. long. There are nine plates per assembly.

The fuel plates are assembled by inserting their edges into 1/16-inch deep grooves in 1/8-inch thick side plates. These plates are formed by extrusion, and the grooves are slotted at intervals along their length to permit plug-welding to the fuel plate edges.

The top and base of the alternate fuel element design are identical to that of the reference design.

3. Control Rods

The "rods" are either full crosses, consisting of four blades joined along a common axis, 14-1/4 in. wide across blade edges, or tees, in which three blades are so joined (see Figs. 4 and 8).

The initial core loading includes five full-cross control rods. The four tee control rod positions will be initially filled with inactive rods of aluminum-nickel sheet. These may be replaced later by active rods containing cadmium.

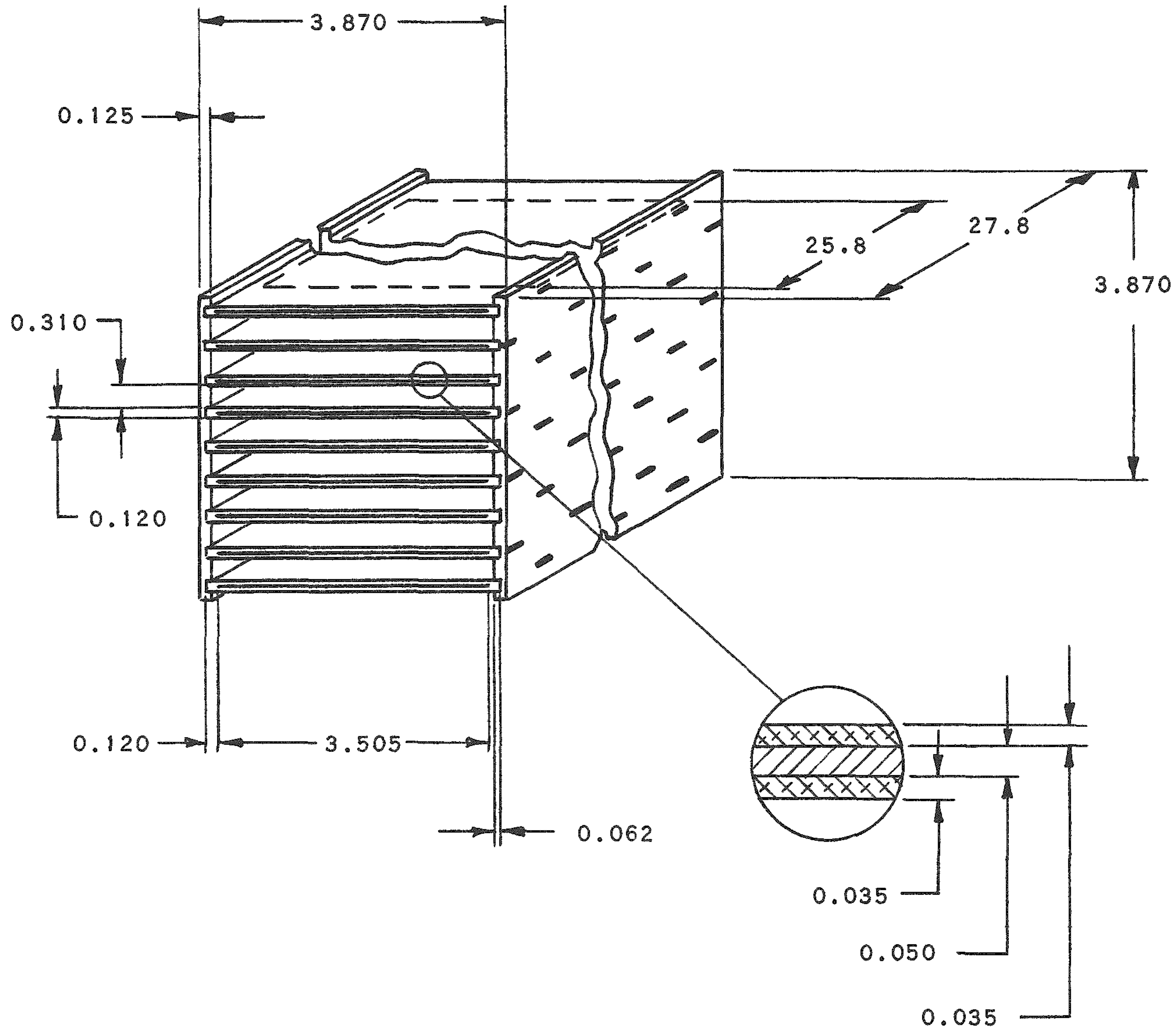

FIG. 6
ALTERNATE FUEL ELEMENT

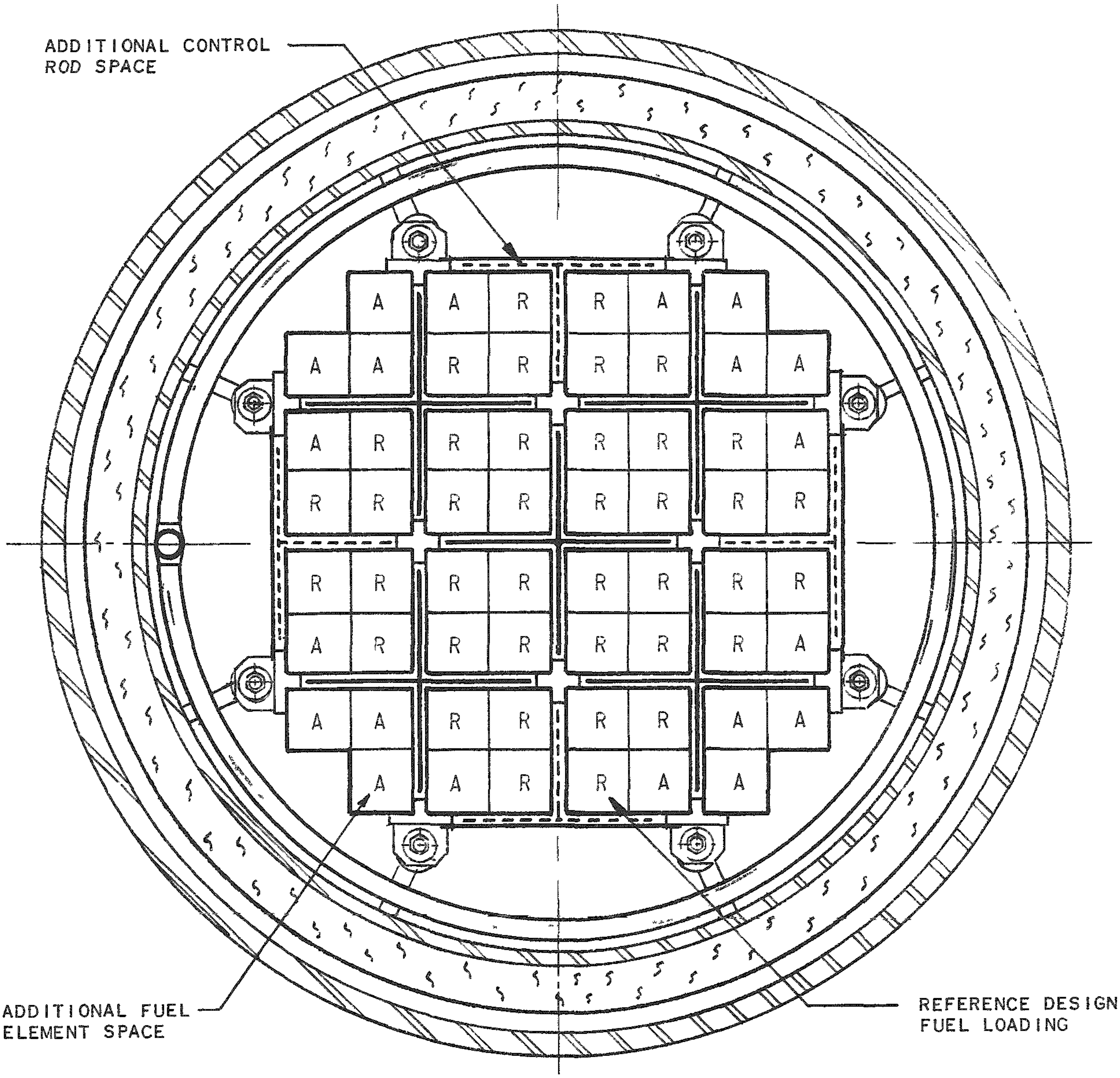

FIG. 7
CORE LOADING PATTERN

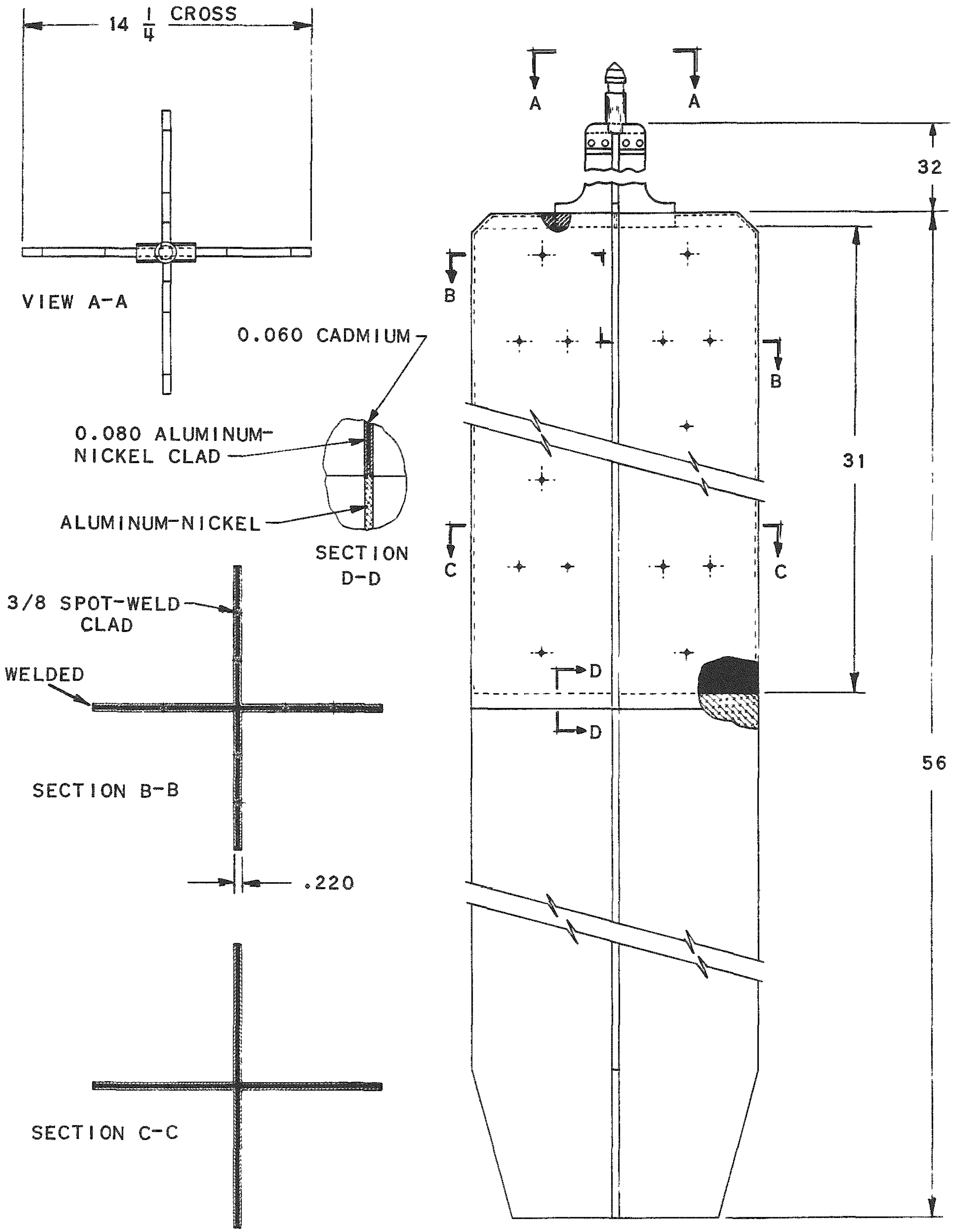

FIG. 8
FULL CROSS CONTROL ROD

a. Construction

Figure 8 shows a full-cross control rod. The active portion of each blade is 0.060-inch thick cadmium sheet, 31 in. long by 7 inch wide. The cadmium is confined between two 0.080-inch thick aluminum-nickel sheets, edge-welded. The cadmium is perforated at intervals by 1/2-inch diameter holes, through which the aluminum-nickel cladding is dimpled and spot-welded to provide support. The over-all length of the control blade is 56 in. The lower following portion, approximately 25 in. long,is made of solid aluminum-nickel plate. A 3 in. x 3 in. solid aluminum-nickel cross-shaped rod extension 32 in. long, is attached to the upper end of the control blade. The over-all length of a complete control rod assembly is approximately 93 in.

b. Operation

The length of cadmium provides overlap beyond the active length of the fuel element.

When fully inserted into the core, approximately all of the follower section extends beyond the bottom of the fuel elements. The follower remains in the control rod channel when the cadmium section is withdrawn from the active zone and serves to reduce thermal neutron peaking in the channel.

A shock absorber and stop arrangement, located within the control rod drive mechanism, functions during rod drops. However, a final positive mechanical stop is provided near the top of the rod extension. This stop would bear against the tops of the shrouds.

B. Control Rod Drives

Two distinctly different types of drives are under experimentation at Argonne National Laboratory. They are: (1) a mechanical drive in the form of rack and pinion (Fig. 9); and (2) an electromagnetic drive in the form of a step linear motor (Fig. 10).

The mechanical drive incorporates the basic concept of transmitting rotary motion into linear motion. In this way a rotary shaft pressure seal can be used in lieu of a reciprocating shaft seal.

The magnetic drive is a unit with no seals other than the static mounting seal. Operation of this drive is by energizing certain coils in sequence to perform the linear motion for actuating the control rods or holding them in position.

Both types of control rod drives can be used for "scramming" the reactor in case of emergency.

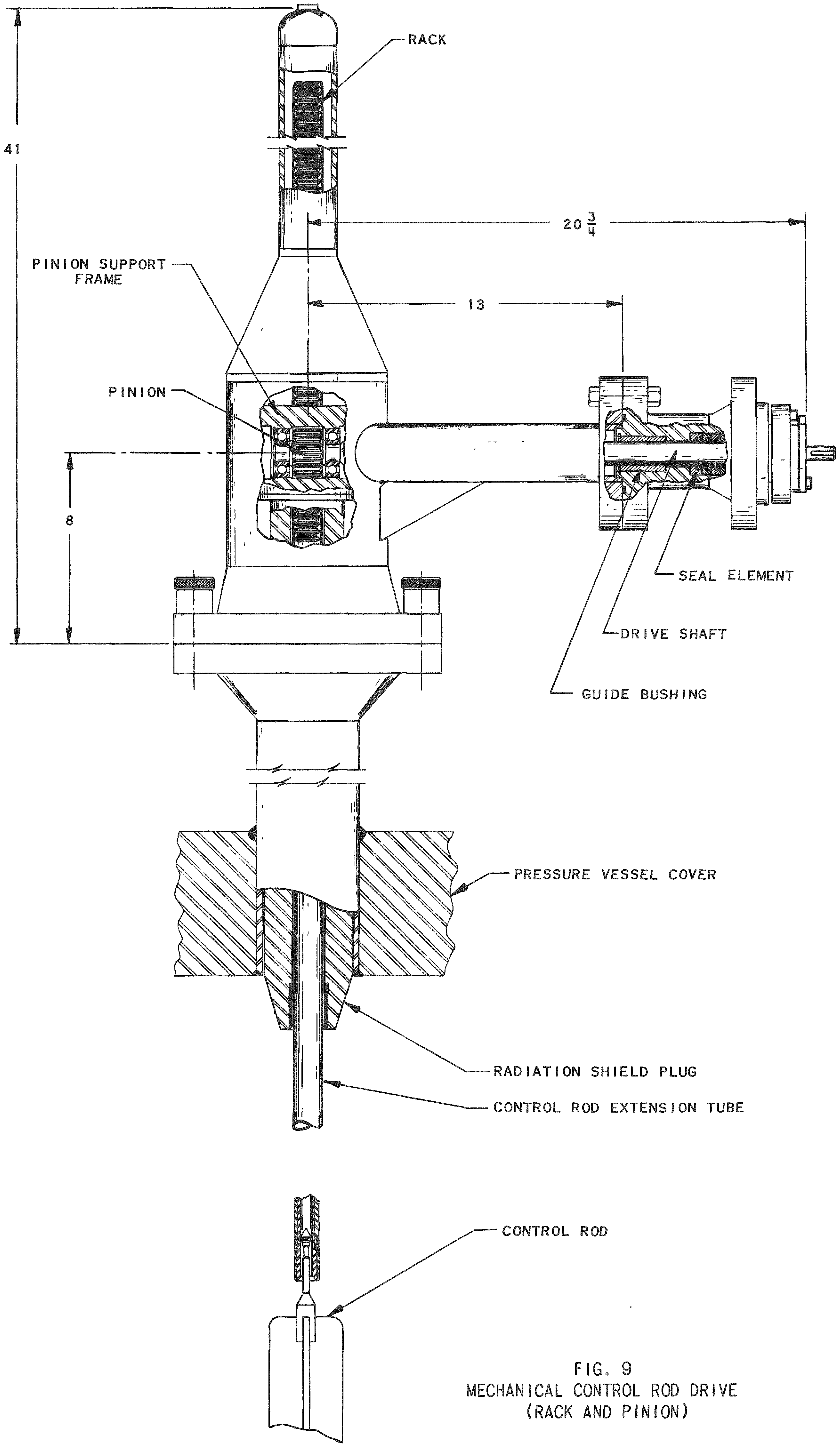

FIG. 9
MECHANICAL CONTROL ROD DRIVE
(RACK AND PINION)

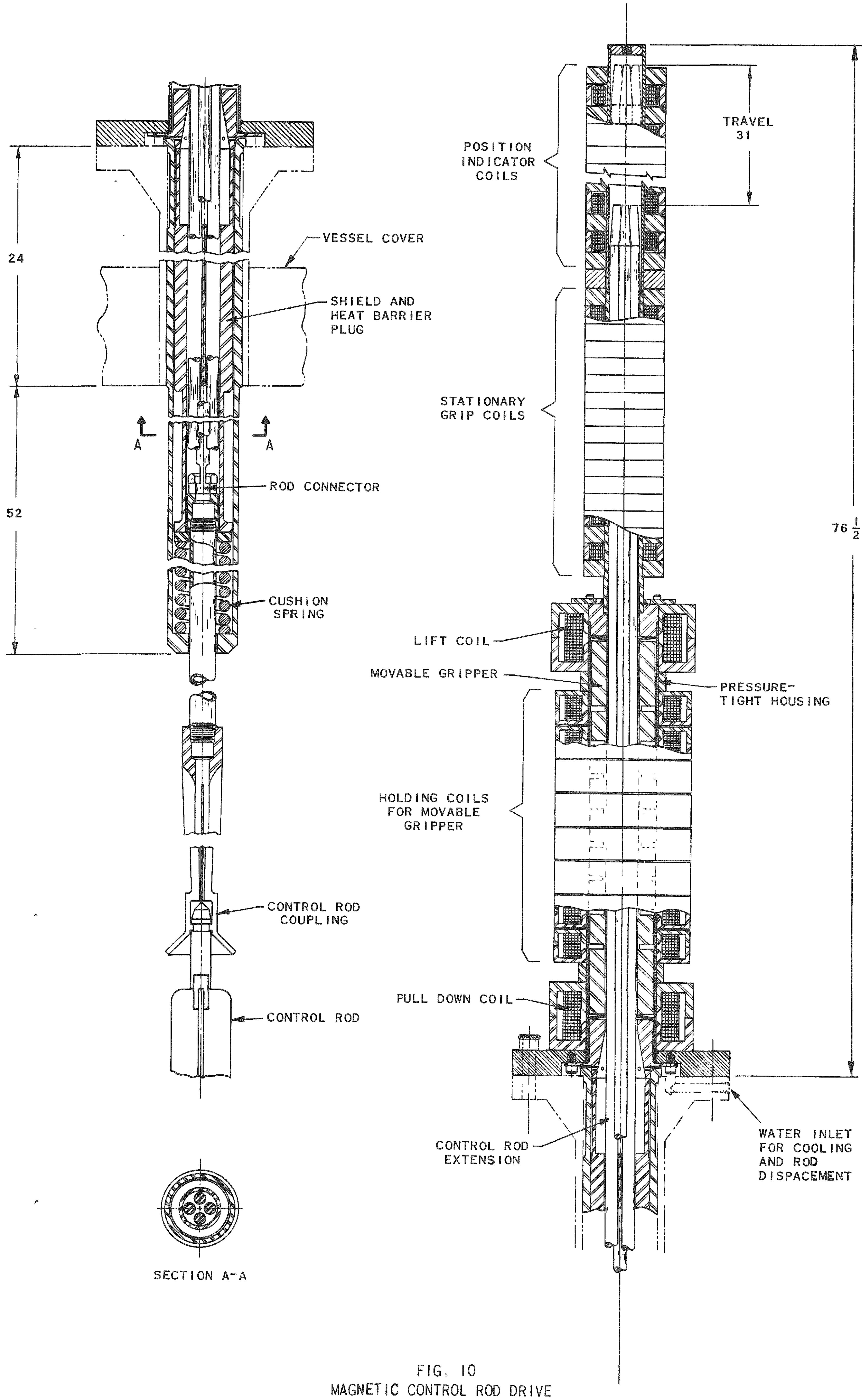

FIG. 10
MAGNETIC CONTROL ROD DRIVE

C. Shielding

1. Description

Since the ALPR differs from previous power reactor designs in its size and final location, various problems of an unconventional nature must be considered in its shield design. Reactor shielding always involves the use of heavy materials and bulky configurations. It is of prime importance in this project to minimize the actual weight of material which must be transported to the reactor site. The main bulk of the biological shield is gravel, locally obtained (Fig. 1). Concrete for movable shielding is poured into forms with angle iron imbedded at the edges to prevent chipping. Local gravel is used as the aggregate. Steel plates for shielding are bolted or just laid in place.

The permafrost situation also dictates limitations on shielding. Radiation heat generation is such that below-ground construction is impractical. The amount of heat generated in the shield is such that a progressive thaw would take place if the permafrost is not insulated from both reactor heat and radiation.

The main biological shield is contained in a cylindrical structure. The radial thickness of the gravel is over 16 ft. About 12 ft of gravel will attenuate the reactor radiation to AEC tolerance level. Thus, the structural design contains more than enough gravel for shielding. Out to a radius of about 6 ft beyond the support cylinder, the space just below the biological shield is filled with gravel placed in the space between the I-beams. Steel plates are placed just below the top of the I-beams and extended two to three feet beyond the outside of the support cylinder. While these plates serve no structural purpose, they attenuate core gamma radiation and cause the resultant heat to be generated well above the gravel pad and permafrost region. The cover of the pressure vessel is a 6-inch steel plate with a boral sheet on the underside. Above this is 3 ft of removable concrete.

2. Main Biological Shielding

In these shielding calculations, standard techniques are employed which at all times reflect a pessimistic point of view. In this report, only results will be summarized.

The reactor core is approximated by a homogeneous sphere of the same average composition as the core itself. Water in the core is taken to be of specific gravity 0.85, and this figure is also used for water in the reflector.

Fluxes of fast neutrons are calculated by removal theory, thermal fluxes by diffusion theory, and gamma ray fluxes using linear buildup.

a. Radial Shielding

Neutron flux levels are calculated along a horizontal radius at the level of the midplane of the core (see Table 4).

Table 4

NEUTRON FLUX LEVELS

Location and Nominal Thickness	Nominal Distance from Centerline (cm)	Neutron Flux, n/(cm^2)(sec) Fast	Thermal
Core outside surface	41.5	8.28×10^{12}	1×10^{13}
Inside surface			
Pressure vessel (1 in. thick)	66.0	6.9×10^{9}	1.5×10^{11}
Support cylinder (1 in. thick)	82.0	2.55×10^{9}	7×10^{10}
Thermal shield (2 in. thick)	87.0	1.1×10^{9}	3×10^{10}
Gravel	92.0	1×10^{8}	1.5×10^{10}
One foot into gravel	122.5	1×10^{7}	3×10^{9}
Three feet into gravel	183.5	-	2.5×10^{7}

Gamma doses are computed using five energy groups. Near the pressure vessel and support cylinder, the heating effect of gamma rays is of primary interest rather than the dose. At 10 ft into the gravel, the gamma dose is 4.4 mr/hr. Since the shield has over 16 ft of gravel, the dosage at the outside is nil. At the top of the shield pile a steel plate covers all of the floor area within three feet of the pressure vessel lid.

b. Axial Upward

Boiling water above the core is taken at specific gravity of 0.5. The water level is approximately five feet above the core. A slab of steel serves as the pressure vessel cover. A sheet of 1/4-inch thick boral is placed just beneath it. The boron-carbide matrix is black to thermal neutrons and minimizes the number of thermal (n-γ) reactions in the iron. This effectively cuts down dangerous gamma radiation above the reactor. At least three feet of concrete are needed above the pressure vessel top to moderate and absorb neutrons and attenuate capture gamma rays from the iron. A particularly important region is the space between the control rod housing thimbles.

A convenient and cheap mixture for shielding in this location is two parts (by volume) sand or fine gravel, one part small steel punchings, and one part boric oxide. This mixture should weigh 200 lb/cu ft or more. B_2O_3 is specified rather than borax due to the hazard from sodium activity and the behavior of borax at high temperature.

The top part of the shield is concrete one-foot thick. The ends of the control rod housings must pass through openings in this layer. The openings should be as small as possible to prevent streaming.

The fast neutron flux in the steel cover is about 10^6 nv at the bottom, dropping by a factor of ten in the plate. The thermal flux is of the order of 5×10^5 down to 10^5 n/(cm^2)(sec). Thermal flux in the concrete drops from 3×10^5 to about 2×10^3 in three feet of concrete (unborated). Along the axis the dose should be less due to the presence of steel and boron. The limiting dose above the concrete consists of capture gamma rays from the iron cover and concrete. The dose above the operating reactor is expected to be about 30 mr/hr of gamma rays (about one third from the pressure vessel lid and the rest from captures in the concrete) plus about 60 fast n/(cm^2)(sec) and about 2000 thermal n/(cm^2)(sec).

This level of radiation is such that a man can spend about seven hours working time per week directly on top of the concrete. Actually, there is very little likelihood that personnel would be required to enter this area during operation.

c. Axial Downward

Below the reactor, space is considered inaccessible. No effort will be made to limit biological dose in the air space. After construction of the prototype, the scattered radiation from the underside of the shield will be surveyed to check for hazards at the outside of the shield.

Shielding below the core consists of about 2-1/2 ft of water, the pressure vessel, 4 in. of steel, and the gravel packed between the I-beams. Mixing a small quantity of borax into the gravel just below the reactor tank would minimize capture gamma rays from the gravel. A thin layer of B_2O_3 is spread on the flat surface above the cooling coils. This serves to hold down captures in the steel. Dose rates of one to ten roentgen per hour will exist in the air gap below the reactor.

3. Heat Generation and Temperatures

Most of the heat generated in the shield is due to gamma rays of medium energy that originate in the reactor core. Heavy materials are the most effective gamma shields and every gamma ray stopped gives up its energy into heat. An effort is made to place heavy material as near to the core as possible to minimize weight requirements and facilitate heat removal. Table 5 is a tabulation of sources of gamma radiation and the resultant heat generation in the shield. Neutron heating and other capture gamma heat sources are negligible.

While this does not seem to be a large amount of heat, the gravel shield is effectively a large insulator. Its thermal conductivity is low [estimated 0.3 to 0.4 Btu/(hr)(ft)(F)] and practically no heat will leave the gravel except by conduction back toward the reactor. With thermal shield placed outside of the support cylinder, about 75% of the radiant energy is absorbed in it, and the remaining radiation will not cause the generation of super-high temperatures in the shield. Cooling between the support cylinder and thermal shield will remove this heat and whatever heat can be conducted back from the gravel. A two-inch steel shield will reduce the heat generation in the gravel to less than five kilowatts.

The shield cooling system is adequate to carry away all radiation heat which is generated outside the pressure vessel in addition to an estimated ten kilowatts of thermal heat leakage. The heat generated in the top, and outside the bottom shielding is not carried in the cooling water, but this amount is negligible. The total heat generated in the top is less than 0.1 kw.

Below the reactor, a total of about one kilowatt of heat is generated below the steel plates. About 90% of this energy is absorbed in the gravel below the steel plates. Thus, energy enters the gravel foundation pad at a rate of less than 0.1 kw. Heat generation in the permafrost itself is of the order of a few watts at the most (calculations indicate less than one watt with a 2-foot gravel pad).

4. Shutdown

Delete

After the reactor is shut down, the pressure vessel is filled with cold water. With a level of 10 ft above the top of the core, the dose rate at the surface two hours after shutdown is about 30 mr/hr. With the cover on the dose rate is nil. Unloading operations are conducted with the cover on so that even with a hot fuel element a few feet above the core no radiation hazard exists outside the vessel. However, workmen must withdraw to at least a ten-foot distance while the element is being drawn up into the coffin. The coffin provides about ten inches of lead shielding for a spent fuel element, reducing the dose at its surface to about 100 mr/hr.

Table 5

SOURCES OF GAMMA RADIATION AND HEAT GENERATION

(In Kilowatts)

	In Core		In Reflector		Total	
Gamma energy production		266		114		380
Energy absorption in core and reflector	213		92		305	
Energy conversion to heat in pressure vessel	27		12		39	
Heat dissipation to reactor coolant		240		104		344
Energy conversion to heat:						
In support cylinder	13		5.3		18.3	
In 2-inch steel thermal shield	10		3.7		13.7	
In gravel	3		1		4	
Heat dissipation to shield coolant		26		10		36
		266		114		380

IV. REACTOR CONTROL

A. Inherent Controls

One of the significant qualities of the Boiling Reactor is the inherent capacity to regulate its power level so as to maintain consistent volumetric steam void in the core. This means that increased bubble formation will cause a decrease in reactivity and power level.

Another feature which can be considered inherent control in case of this reactor is the boron burnout. This burnout of poison, along with the burnout of fuel, controls the reactivity to a certain degree, by reducing the changes which would otherwise take place during the life of the fuel core.

B. Demand Control

The ALPR specifications call for a control system which ties the reactor power level to the electric demand so as to minimize waste of fuel.

On the other hand, steam must be available for a considerable instantaneous increase of electric demand. For this reason a system has been chosen which involves a steady bypass flow of steam, as much as 16% of the normal production. This bypass flow will be ready for use in the turbine in case an additional load of as much as 60 kw should suddenly be added to the electric demand.

The change in the bypass will then signal back to the reactor control system which will automatically adjust the power level until the normal bypass flow rate is re-established. The turbine operation is to be stabilized in less than 5 sec, but in order to maintain safe reactor operation, the buildup of reactivity will be extended over about 25 sec for a 60-kw step, after which an additional step of equal magnitude can be allowed in the power demand.

It should be noticed that the bypassed steam will be utilized in the space-heating system during the greater part of the year and only a fraction of the heat will go directly to the condenser.

The changes in reactivity called for by the steam demand are taken care of by two alternate systems. One is the control rod system consisting of five cadmium cross rods. One or more of these rods are used for operating control; the others are adjusted as shim rods. The rods also serve as "scram rods." The other system is intended to more or less relieve the work done by the power-driven control rods. It is a feedwater preheat system similar to one described in ANL-5452, based on the principle that feedwater can be returned either directly to the reactor core, where it will subcool the moderator water, or into the steam dome, where it condenses some of the steam and is preheated to saturation temperature before entering the reactor core. The reactor power will be dependent on the ratio of feedwater entering the reactor through either of these two inlets.

The signal to the feedwater valves will be coordinated with the signal from the turbine governor to the throttle valve, whereby the reactor adjustment can be started immediately as the power demand changes. The value of this feedwater control system can only be determined by actual operation of the prototype plant.

V. FUEL LOADING AND UNLOADING

The procedure and equipment described herewith are for the purpose of unloading a hot reactor core and reloading with new fuel elements (Fig. 11). The initial cold core can be installed with a simple procedure before the pressure vessel cover is installed. The reloading is accomplished without removing the pressure vessel cover, thereby leaving the gasketed seal intact.

Preparation for reloading the core can commence immediately after reactor shutdown; the extent of this preparation is limited by the time necessary to bring the reactor pressure to zero and raise the reactor water level to a height immediately below the pressure vessel cover. The water introduced for shielding purpose will come from, and return to, a retention tank (reactor contaminated water storage). All piping and components will be selfdraining. Preliminary preparation for reloading will, furthermore, consist of disconnecting the motors and control rod drives to an extent that does not break any pressure seal to the reactor. Shielding above the reactor and around the control rod drives can also be removed during this period to the extent dictated by the radiation level. Upon establishing zero reactor pressure and full water level, the rest of the top shielding is removed and the control rod drives are taken from the reactor. The rod drive extensions will be disconnected at the rods and removed from the reactor. This leaves an unobstructed passage from under the pressure vessel cover to the core over the entire area of the core.

The central control rod thimble is designed to receive an adapter to the fuel element coffin and also carry the full load even though the crane will carry the major portion. The other control rod thimbles are utilized by a periscope, a fuel element manipulator, and also for an underwater lighting access port (Fig. 11). Caps are placed on those thimbles which are not in use. The procedure for unloading a hot fuel element is as follows: With the periscope, manipulator, and lighting in position, the coffin (Fig. 12) is placed on the central rod thimble adapter. The coffin fuel element gripper is lowered into the reactor by a hoist until it is immediately above the core shrouds. The manipulator takes hold of the upper part of the coffin gripper and attaches it to the fuel element selected. The manipulator extracts the fuel element from the core and moves it to the centerline of the coffin. At this point in the procedure, the personnel will stand back and one operator will use the hoist crank that operates the hoist through a long flexible shaft. Indication that the fuel element is in the coffin is made by means of an indicator on top of the coffin. The personnel may then return and the coffin gate is closed. The coffin is then transported to the fuel storage hole by means of the crane and unloaded there, then returned to the reactor for another fuel element. The above procedure is repeated until the fuel elements designated have been removed.

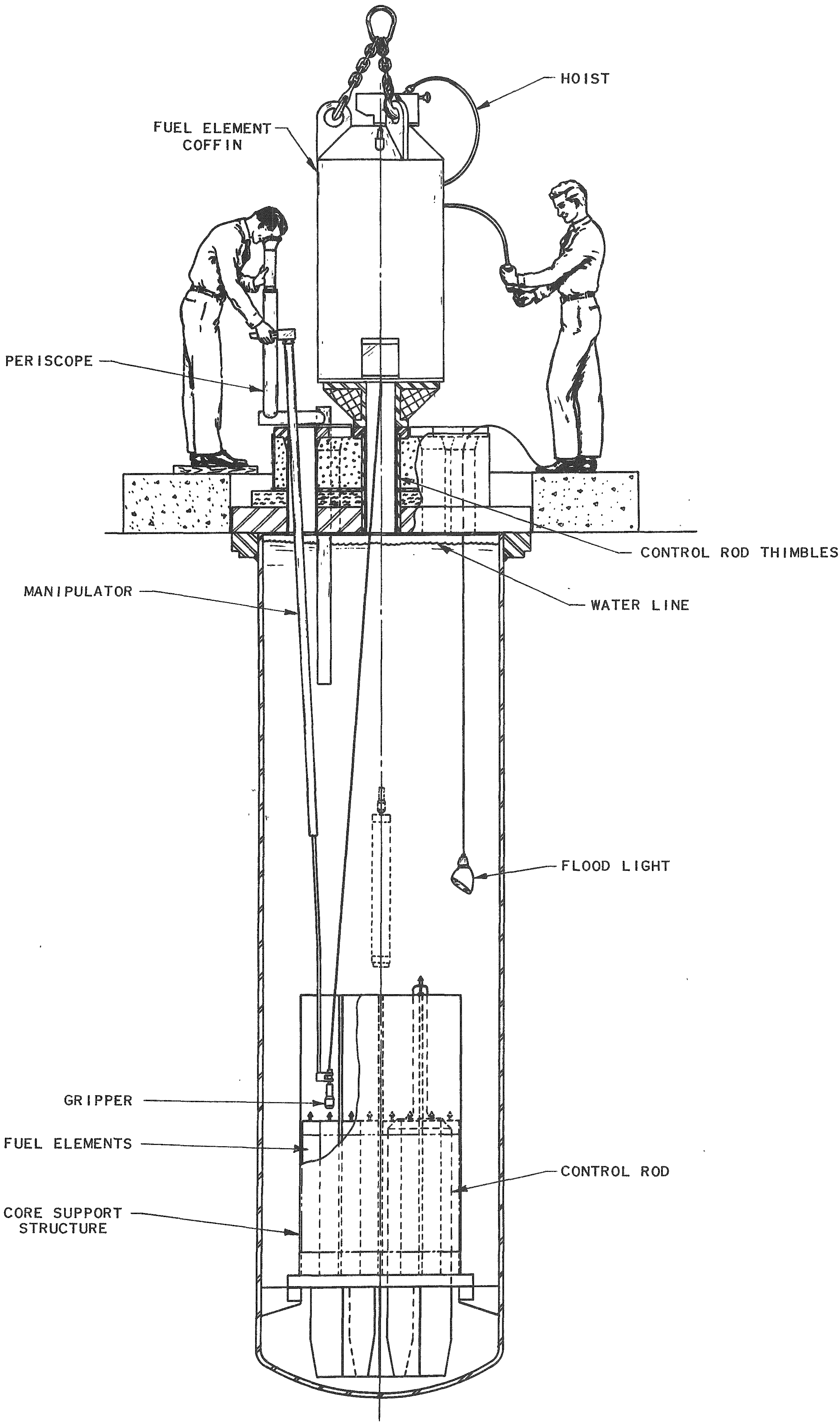

FIG. 11
FUEL ELEMENT TRANSFER SYSTEM

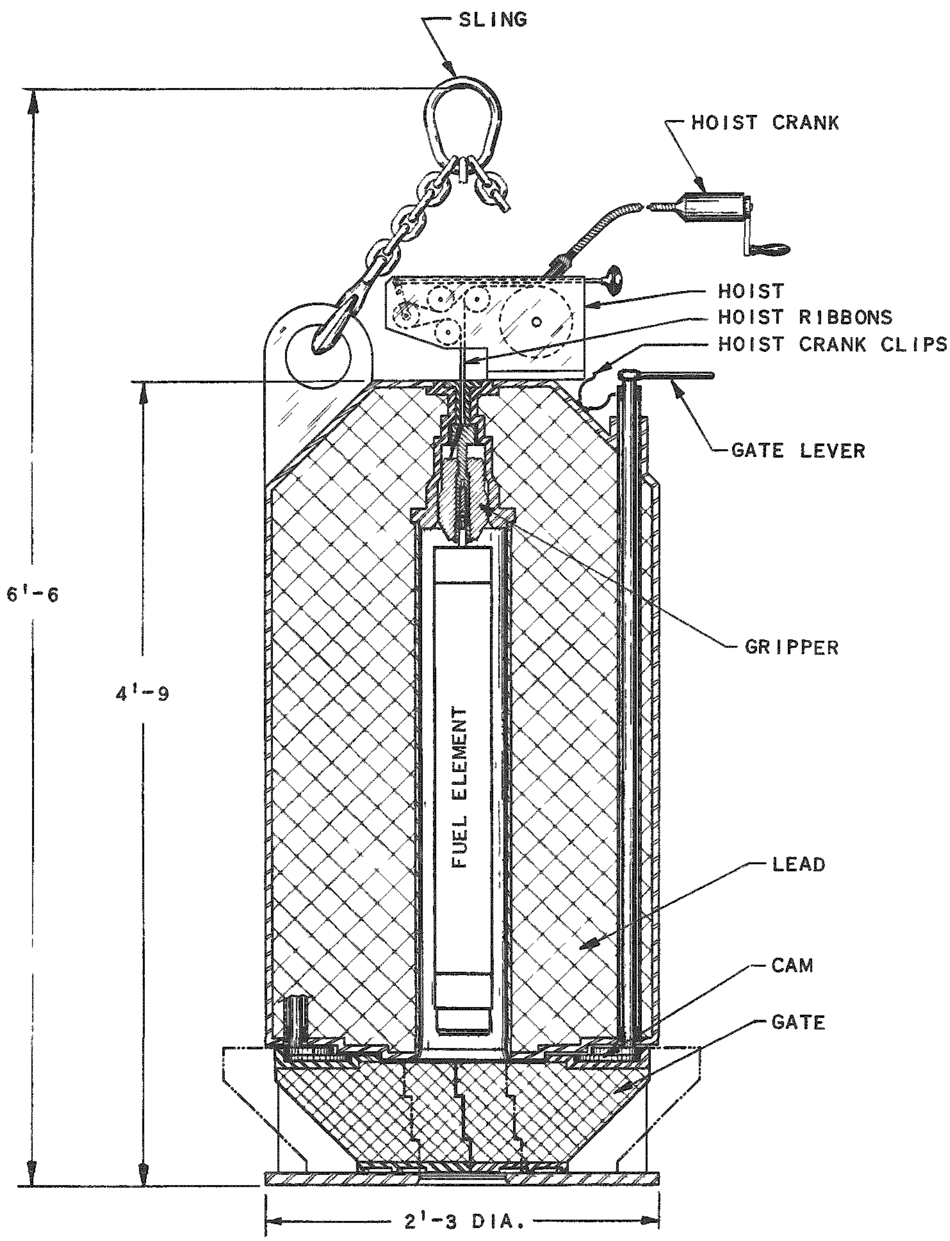

FIG. 12
FUEL ELEMENT COFFIN

The loading of cold fuel elements is accomplished by the above procedure in reverse, but without the coffin. The cold fuel element is lowered into the reactor through the central thimble until it is immediately above the core shrouds. The manipulator then takes hold of the fuel element gripper and places the element in the position designated. The fuel element gripper is released and the procedure repeated for subsequent cold fuel elements.

After reloading the core, the units disassembled are reassembled and the water level in the reactor tank brought down to operating level.

VI. CORROSION AND WATER PURIFICATION

In this section are summarized the available experimental information applicable to ALPR prototype operation, as it affects corrosion and related problems. The principal interest is in the use of aluminum-nickel in the reactor core; but the corrosion problems of all components of the ALPR plant are at least briefly considered. It is generally concluded that the use of aluminum-nickel in the core and stainless steel in other susceptible locations leads to corrosion rates that are acceptably low. Fouling of heat transfer surfaces is not serious. No unusual problems arise from corrosion of radioactive metals.

A. Survey of Flow System

The main features of the flow circuits are shown schematically in the simplified flow diagram (Fig. 13). The materials of construction are summarized in Table 6.

Table 6

MATERIALS OF CONSTRUCTION

Item	Material
Core	Aluminum-nickel
Pressure vessel	Type 304 stainless steel
Steam separator	Type 304 stainless steel
Piping to turbine (as well as all other piping that contacts high temperature reactor water)	Type 304 stainless steel
Turbine	Casing: carbon steel; shaft: 1% Cr-1/2% Mo steel; buckets, diaphragm vanes, bands, and nozzles: 13% Cr steel; diaphragms: cast iron; wheels: 1% Cr steel.
Condenser	2S aluminum
Feedwater pump	18-8 Stainless steel
Filter housing	18-8 Stainless steel
Ion-exchange resin containers	18-8 Stainless steel

RE-8-17128-A
H.PEARLMAN:W.K.,1-11-56

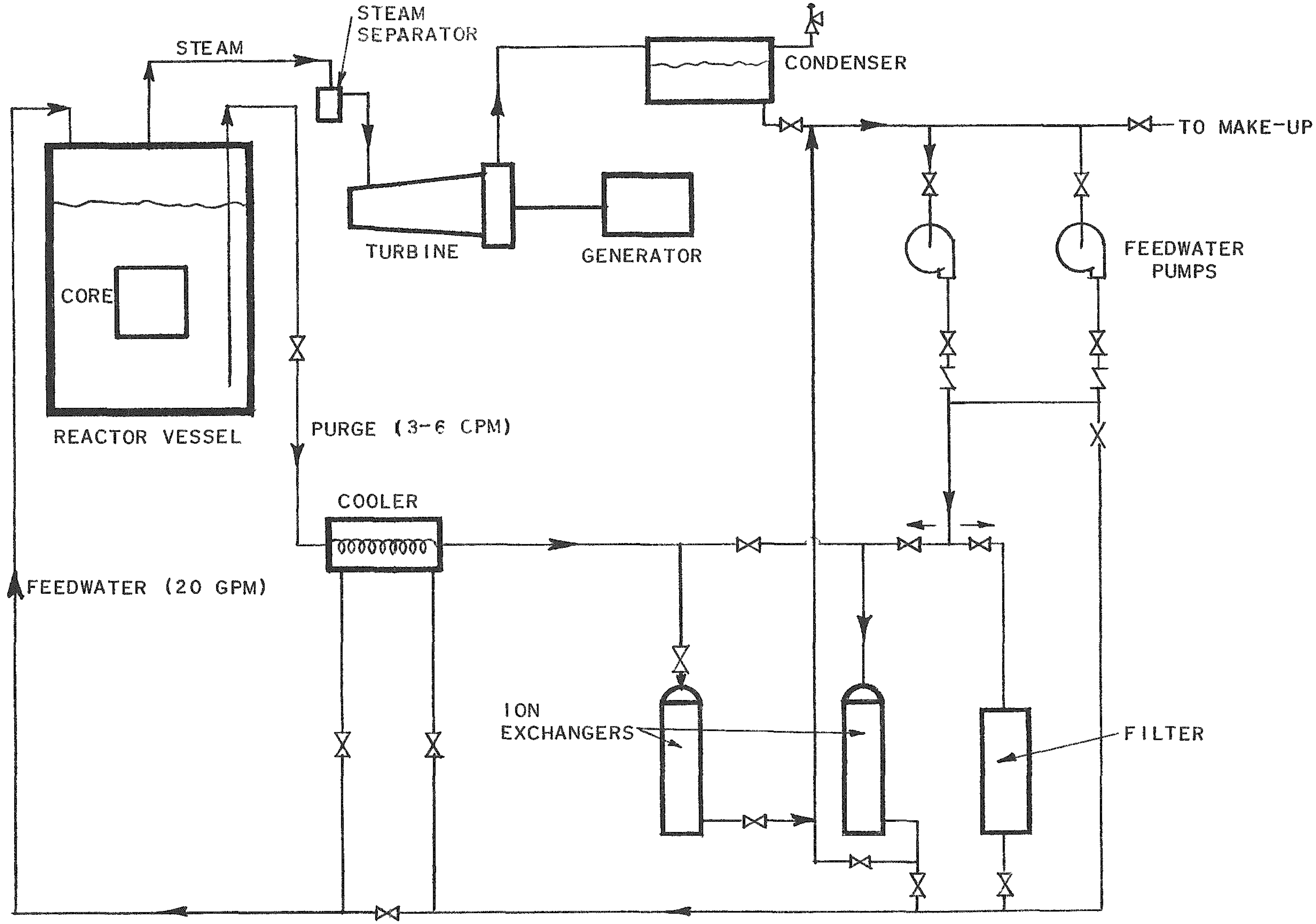

FIG. 13
SIMPLIFIED ALPR FLOW DIAGRAM

Aluminum-nickel has been chosen as a structural or cladding material for all core components because it is inexpensive, adequately strong, easy to fabricate and appears to have excellent resistance to corrosion. In addition, its nuclear properties compare favorably with other feasible structural materials.

The average penetration rate of aluminum-nickel due to corrosive attack under operating conditions is estimated to be 1 mil/yr. Over the three-year core reloading period specified, this corrosion rate would have an insignificant effect on structural components. The part most vulnerable to corrosion is the 0.030-in. or 0.035-in. thick cladding on the fuel elements; this would appear to be safe even if the stated rate were exceeded by a factor of 5.

In the plant the maximum temperature and pressure 417F (214C) and 300 psia, respectively are found in the pressure vessel. The steam rate is about 8500 lb/hr, corresponding to a feedwater return rate of about 20 gpm. Piping and other components are sized to limit linear fluid velocities to moderate rates.

Under the above conditions, corrosion rates of stainless steel will be negligible. For example, short-time exposures(1) of static steam-water mixtures in type 347 stainless steel containers under mixed reactor radiations at 500F indicate an average penetration rate less than 0.1 mil/yr. Long-duration experiments on dynamic pressurized water systems in type 304 or 347 loops at 30 fps velocity, indicate a corrosion rate of 0.08 mil/yr at 500F.(2)

Corrosion rates in the 2S aluminum condenser and in the low alloy steel feedwater pump housing are also expected to be acceptably low because of low water temperature, about 135F, in these components.

Experience with turbines operating with saturated 300 psia inlet steam in direct cycle boiling reactor plants is limited to BORAX III. Operating schedules on the BORAX III have so far not permitted direct observation of turbine corrosion. In the absence of such observations, there is no basis for reliable prediction of corrosion in the ALPR turbine. If later BORAX-III observations indicate that better corrosion resistance is required than is provided by the standard turbine materials listed in Table 6, it appears possible to apply surface coatings, such as chemically deposited nickel-phosphorus,(3) to turbine components to provide improved performance.

In summary, there appears to be no corrosion problem in the sense of excessive metal removal. Two other possible corrosion phenomena, besides metal removal, are: first, deposition or crudding on heat-transfer surfaces,(2) such as hydrous magnetite on aluminum-nickel; secondly, "freezing" of valves and similar components that, although movable, may remain in fixed positions for varying periods of time, up to three years.

The two latter phenomena, as well as metal removal, are strongly influenced by the pH, conductivity, and other water properties.[2]

B. Expected Performance of Aluminum-Nickel in the Core

Use of aluminum-nickel in reactor systems was first suggested by Draley and Ruther.[4] Static corrosion data (weight losses determined from stripped samples) are summarized in Fig. 14.[5]

In operation, the reactor core at 300 psia and 417F, aluminum-nickel will be exposed to the following additional conditions: heat flux (metal-to-water), 15,000 to 40,000 Btu/(hr)(ft^2), with boiling occurring over a portion of the heat transfer surface; radiation field, approximately 10^8 rep/hr; water velocity along fuel element surface, approximately 2 ft/sec.

There are no experimental data available under conditions that exactly reproduce ALPR operation. However, in addition to the static corrosion data of Fig. 14, information is available on dynamic corrosion in the absence of radiation; corrosion in boiling systems in the absence of radiation; and also corrosion in pressurized water loops exposed to high radiation fields in the MTR.

1. Unirradiated, Dynamic Corrosion Experiments

Samples of aluminum-nickel were exposed in pressurized water loops over a range of temperature and pH for a period of eight weeks. Results are summarized in Table 7.

It is evident that the corrosion rate increases with increasing velocity. ALPR velocities should lie between 0 and 7 fps.

The corrosion rate is also less at pH = 5 than at pH = 7.

2. Unirradiated, Boiling Corrosion Experiment

An internally heated aluminum-nickel sample was prepared by applying a cladding of aluminum-nickel sheet to a 3/8-in. OD stainless steel tube. The sheet was welded and then drawn tightly. Water at about 500-550F was circulated through the stainless steel tube. The aluminum-nickel cladding was surrounded by a water annulus about 1-1/2 in. wide, enclosed in a type 304 stainless steel vessel. The surrounding water boiled at 417F and 300 psia, which conditions were controlled by a condenser in the steam phase above the boiling water. Water purity was initially maintained by purging, but after 177 hr (see Table 10) a sidestream was pumped intermittently through a mixed-bed ion-exchange column. Heat transfer through the aluminum-nickel varied from 15,000 to 40,000 Btu/(hr)(ft^2) along the tube, with an average of 25,000 Btu/(hr)(ft^2).

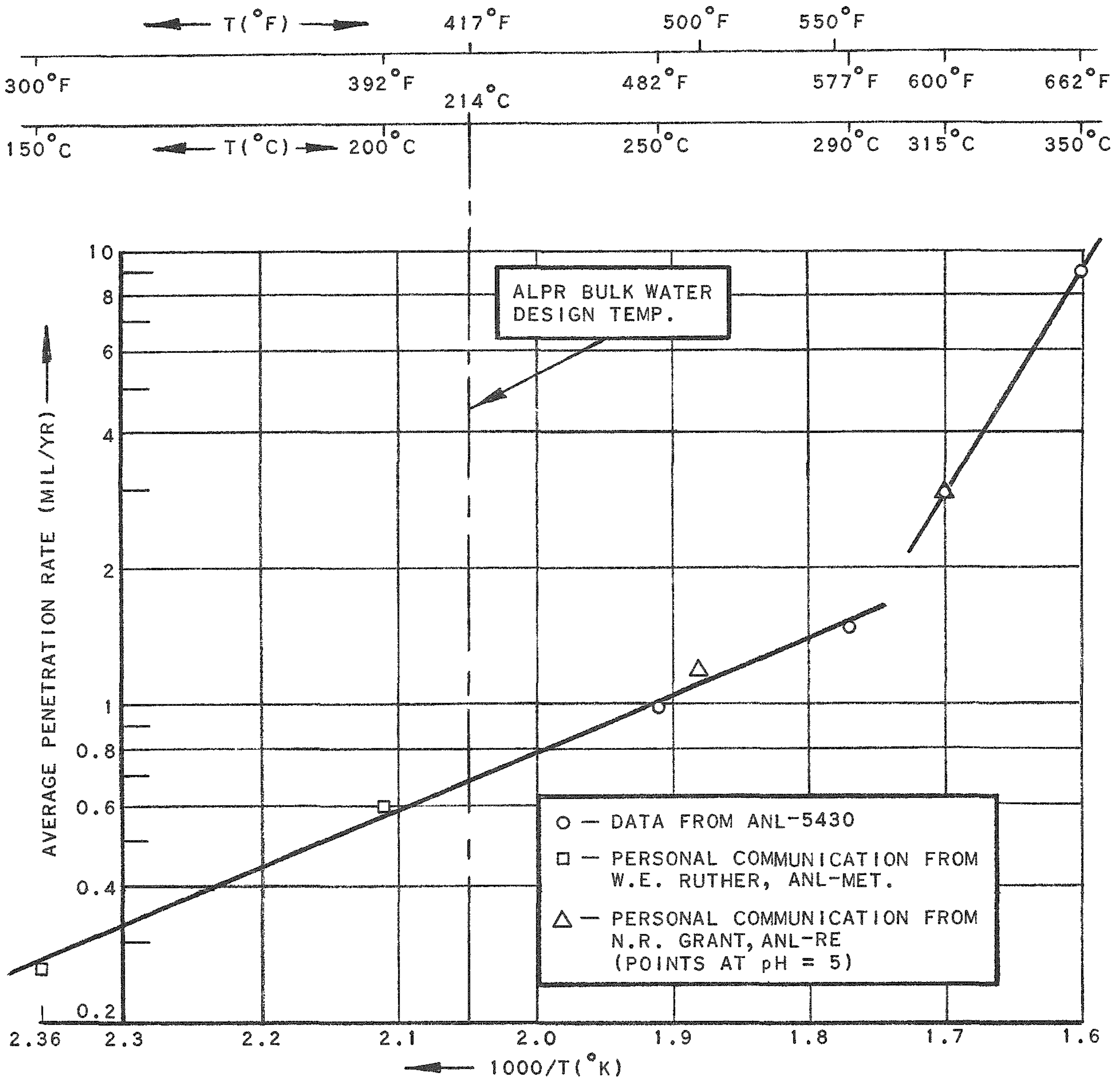

RE-7-17121-A

FIG. 14
TEMPERATURE DEPENDENCE OF
Al-Ni STATIC CORROSION RATE

Table 7

DYNAMIC CORROSION OF ALUMINUM-NICKEL, UNIRRADIATED[6]

Temp. (F)	Flow (fps)	pH	Average Penetration[a] (mils/yr)
500	static	5	1.2
500	7	5	1.3
500	18	5	2.1
500	static	7	1.3
500	7	7	1.7
500	18	7	1.5
600	static	5	3.0
600	7	5	5.4
600	18	5	7.3
600	static	7	5.3
600	7	7	6.2
600	18	7	8.8

Notes: [a] Determined from weight losses on stripped samples. Each value is the average of several samples.

Results are summarized in Table 8. In general, the aluminum-nickel was in excellent condition after the 1702-hr exposure.

3. Dynamic Corrosion Experiments in MTR

Aluminum-nickel sample plates were exposed in a dynamic loop in the MTR. Unirradiated samples were exposed to the same temperature, pH and flow conditions as controls. Despite lack of constancy of the experimental conditions (especially the temperature), it appears clear that the corrosion rate is lower under irradiation by a factor of about 3. The results are summarized in Table 9.

Table 8

UNIRRADIATED BOILING EXPERIMENT

Hr	Wt Gain (mg/cm^2)	Diameter, In. Exposed to Water	Diameter, In. Water and Steam Junction	Diameter, In. Exposed to Steam	Appearance
0		0.5002	0.5002	0.5002	Metallic
170	2.22	0.5008	0.5014	0.5004	Water: Typical Al-Ni adherent grey coating. Junction: Slight reddish coloring, probably iron oxide. Steam: Adherent dull white-grey coating.
1083	1.61	0.5012	0.5014	0.5003	Water: Adherent red coating with a few, very small spots of bare metal along scratches in tube. Junction: Adherent red coating. Steam: Adherent dull white-grey coating with a little red coloring near junction.
1702 Before strip	1.98	0.5012	0.5014	0.5005	Water: Adherent red coating with more of the very small spots of bare metal showing. Junction: A band of darker red coating. Steam: Adherent dull white-grey coating with a little red coloring near junction.
After strip	-3.95	0.4996	0.5000	0.5002	Dull metallic appearance.

Table 9

CORROSION OF ALUMINUM-NICKEL UNDER IRRADIATION[6]

Series A:

Temperature: 300 to 500F
Flow: 30 fps
pH: 6.2 to 7.8
Water Resistivity: 0.3 to 3.0 megohm-cm
Exposure: 1250 hr

Approx. ϕ_{th},[a] n/(cm^2)(sec)	Weight Loss[b] (mg/cm^2)
Approx. 10^{14}	3.6
Approx. 10^{13}	5.3
Unirradiated	19.5

Series B-1:

Temperature: 485 to 500F
Flow: 30 fps
pH: Approx. 7
Water Resistivity: Approx. 1 megohm-cm
Exposure: 200 hr

Approx. ϕ_{th}, n/(cm^2)(sec)	Weight Loss (mg/cm^2)
Approx. 5×10^{13}	3.0
Unirradiated	8.9

Series B-2:

Temperature: 485 to 500F
Flow: 30 fps
pH: Variable. Two observations gave 7.4 and 8.5.
Water Resistivity: Variable, as low as 0.01 megohm-cm.
Exposure: 340 hr.

Approx. ϕ_{th}, n/(cm^2)(sec)	Weight Loss (mg/cm^2)
Approx. 5×10^{13}	7.8
Unirradiated	11.2

Series B-3:

Temperature: 485 to 500F
Flow: 30 fps
pH: Variable, but mostly near 7.
Water Resistivity: Variable but mostly near 0.2 megohm-cm.
Exposure: 540 hr

Approx. ϕ_{th}, n/(cm^2)(sec)	Weight Loss (mg/cm^2)
Approx. 5×10^{13}	4.7
Unirradiated	13.2

Notes:
(a) Fast neutrons and gammas were also present. The thermal neutron flux is intended to indicate the general level of radiation.

(b) Weight loss only. Data do not permit estimate of corrosion rate. Each value is average of measurements on four samples.

4. Surface Fouling

Although no experiments have been designed specifically to test surface fouling on aluminum-nickel, some pertinent information is available from the boiling corrosion experiment. The average temperature drop across the tube wall was calculated from measurements made throughout the duration of the experiment. Data are summarized in Table 10.(7)

Table 10

AVERAGE TEMPERATURE DROP ACROSS TUBE WALL

Exposure (hr)	Average ΔT (F)	pH	Resistivity (megohm-cm)
0	40	6.5	0.5
3	42	6.9	0.13
7	59	6.8	0.13
9.5	69	-	-
12.5	69	7.2	0.3
15.5	60	-	-
17	58	-	-
177	58	6.5 - 7.0	0.13
388	60	6.5 - 7.5	0.2
1031	61	6.5 - 7.3	0.3
1343	62	6.5 - 7.2	0.4
1612	63	6.5 - 7.2	0.4

It is concluded that the surface fouling reaches a steady value after an initial operating period and maintains this value provided water conditions are favorable. The sensitivity to water conditions is apparent from variation in ΔT before and after 177 hours exposure.

5. Galvanic Corrosion

Corrosion between aluminum-nickel and 18-8 stainless steel in contact appears to be negligible. In one experiment,(8) sample plates of aluminum-nickel were bolted in a type 347 stainless steel assembly and exposed in distilled water for 25 days at 600F (315C). No significant effects were noted. In another experiment, a tapered aluminum-nickel plug was bolted in a type 304 stainless steel conical seat with a spring-loaded bolt that exerted about 3 psi holding force. The assembly was immersed in initially demineralized water (pH 6 to 7) at 414F (212C). After 44 days, there was no seizing between the tapered aluminum-nickel and the stainless steel.(9) Final pH was about 7.5.

6. Summary

From the available data, it is concluded that the average penetration rate for aluminum-nickel in the ALPR will be about 1 mil/yr. To achieve this low value, water conditions of pH $\approx$ 6.5 and resistivity $\approx$ 0.3 to 0.5 megohm-cm should be maintained.

Surface fouling and corrosion between dissimilar metals should cause no difficulty.

C. Radioactivity in the Flow System

Water in the core is expected to contain dissolved radioactive species such as N-16, Al-28, Fe-55, Fe-59, Ni-59, Ni-63, Ni-65, and Co-60.[10] Shielding requirements associated with the handling of these activities are discussed elsewhere in the present report. Distribution of radioactivity external to the pressure vessel may occur by two routes: spray entrainment in the main steam circuit (see Fig. 13); and deposition in the side stream water purification circuit, especially on the ion-exchange resins. In this section, primary consideration is given to the radioactivity carryover of dissolved ions that arise from corrosion.

1. Radioactivity Processes in the Main Steam Circuit

a. Steam Decontamination Factor

A program of laboratory experiments and field observations on the BORAX-III plant has been directed toward determination of the decontamination factor (DF) for condensate.[11] The DF is defined as the ratio

$$\frac{\text{(counts/min-ml) in reactor water}}{\text{(counts/min-ml) in steam condensate}} .$$

The observed DF's are in the range 10^3 to 10^4.

b. Radiation Levels in the BORAX-III Plant

Direct measurements have been made of radiation levels at various locations in the BORAX-III plant during operation. Results are summarized in Table 11. The BORAX-III locations correspond roughly to those indicated for the ALPR plant in Fig. 13. The measurements were made with survey meters, in contact either with metal or with the surface of the thermal insulation on the metal, at the indicated locations. The insulation is approximately 3 in. thick. In the case of hotwell activity, a duplicate reading was obtained from a permanent recording instrument. From this, the readings appear accurate within a factor of two.

Table 11

RADIATION SURVEY OF BORAX III[12]

Date (1956):	February 5	February 4	February 11	March 15	February 9
Time:	2235	1930	1745	1900	1400
Reactor Power (mw):	4	8	8[a]	8[b]	14
Location					
Steam line to separator	95-200 mr/hr	240-440 mr/hr	90-160 mr/hr	55-120 mr/hr	0.8-1.6 r/hr
Steam separator, bottom	13	60	29	-	-
Turbine, inlet to steam chest	38	145	55	30	0.45 r/hr
Turbine, outlet casing	12[c]	50	20	15	0.16 r/hr
Condenser, bottom	15-25	130-90	47-80	-	-
Air ejector, line from condenser	70	440	160	80	-
Hotwell, top	44	350	130	-	-
Hotwell, (recorded by permanently located instrument)	55	350	60	-	2.6 r/hr
Water conditions:					
pH	5.6	5.7	6.7	8.1	5.25
Resistivity (megohm-cm)	0.25	0.27	0.49	0.15	0.17

Notes: (a) Just prior to this set of measurements the reactor water was specially cleaned up by passage through an anion-resin exchanger. Normal sidestream purification in BORAX III is through cation and mixed bed resin exchangers.

(b) This set of measurements taken after deliberate addition of KOH to reactor water to raise pH.

(c) Measurement made at this location one day after reactor shutdown indicated 1 to 2 mr/hr.

The 4-mw data provide order-of-magnitude estimates of activity to be expected in the ALPR plant at full power (3 mw), neglecting reduction in radiation fields that may result from any additional shielding provided in the ALPR plant. The BORAX-III plant is essentially unshielded, except for the reactor itself and the ion-exchanger columns.

The influence of water conditions is apparent. Lower activities are observed for the February 11 run at 8 mw, when the pH and resistivity were 6.7 and 0.49 megohm-cm, respectively, than for the February 4 run when these values were 5.7 and 0.27. Raising the pH to 8.1, as in the March 15 run, results in reducing the activity although the resistivity is also reduced. (However, there is no experience with operation of aluminum-nickel at this pH over extended period.) Increasing the reactor power from 4 to 8 to 14 mw (runs of February 4, 5, and 9) increased the activities in more than linear ratio. For example, the hotwell activity increased by a factor of 50 in going from 4 mw to 14 mw.

2. Radioactivity in the Water Purification Circuit

The activity to be expected in ALPR ion-exchange resin columns, resulting from collection of radioactive ions produced by corrosion processes, has been estimated[10] to be of the order of millicuries for short-lived Al-28 and microcuries for long-lived Co-60.

No data are yet available for BORAX-III ion-exchange columns operating under conditions similar to ALPR. Table 12, however, summarizes observations on the BORAX-III cation resin column for operation at 14 mw. By inference from the variation in activity with power level in Table 11, the values shown in Table 12 would have to be reduced by a factor of the order of 10 to approximate 3-mw operation. The factor may be as large as 50.

The BORAX-III cation resin ion-exchange column is about 8 ft high. There is a water space approximately 1 ft long at the top of the column, above the cation resin portion. Water flows downward in the column.

It is evident from Table 12 that much of the water-borne activity is removed by the cation-resin exchanger.

The decay by a factor of approximately 100 in nearly 100 hr indicates an average half-life of about 14.5 hr. This coincides closely to the 14.9-hr half-life of Na-24.

Table 12

RADIATION SURVEY OF BORAX-III ION EXCHANGE COLUMN[a]

Date (1956):	February 9	February 22
Time:	1510-1525	1430
Condition:	Operating	(b)
Power (mw):	14	0
Location		
Top of cation resin	80 r/hr	800 mr/hr
1.5 ft from top	330 r/hr	2700 mr/hr
3 ft from top	56 r/hr	440 mr/hr
4 ft from top	16 r/hr	200 mr/hr
5 ft from top	8 r/hr	120 mr/hr
6 ft from top	4 r/hr	80 mr/hr
7 ft from top	3.9 r/hr	40 mr/hr

Notes: [a]All measurements made 6 in. to 8 in. from wall of ion exchange column.

[b]Shut down since 1310 on February 18, following operation at 14 mw.

3. Summary

From the above discussion, it is concluded that radioactivity arising from corrosion should not require shielding on piping and components external to the reactor vessel, except on the ion-exchange column. Extrapolation from BORAX-III data indicates that in the ALPR plant activities will range from 10 to 100 mr/hr on contact with piping and components and may be about 10 r/hr at the cation resin exchanger.

VII. NUCLEAR INSTRUMENTATION

This section outlines the nuclear instrumentation that will be employed to control the reactor, to couple the reactor to the steam system, and also to indicate radioactivity levels at various locations in the reactor plant. Figure 15 is a block diagram of the console instrumentation and related circuitry. Table 13 contains a summary of the principle components of the instrumentation system. It is emphasized that the system as described here relates to the prototype plant. It is expected that substantial simplification of the instrumentation will be possible, as a result of experience gained from operation of the prototype.

As is indicated in Fig. 15, a total of five B^{10}-lined ion chambers are employed. Three of these are uncompensated, and the remaining two are gamma compensated. Of the uncompensated chambers, one feeds through an amplifier and a movable-contact relay to a multirange indicating microammeter on the control console. This channel will be useful during startup and initial operation. Another uncompensated chamber feeds through movable-contact relay directly to a single-range microammeter. This channel will furnish information at high power levels of operation. It will also be useful during "blind" startups. The third uncompensated chamber feeds directly to a galvanometer that indicates power level at the console.

The two-gamma compensated, B^{10}-lined ion chambers feed respectively a linear amplifier and a log amplifier whose outputs are recorded. The log N signal is differentiated to obtain a signal proportional to the reciprocal of the reactor period, and this is displayed on a meter at the console.

The remaining two ion chambers are uncompensated, BF_3-filled units that feed through pulse amplifiers to scaler-counters. These channels provide information useful in startup.

In addition to the recorders and indicating meters described above, the instruments grouped at the control console would include position indicators for the control rods, and meters to indicate radioactivity levels at the following locations (among others): air ejector; hotwell; contaminated waste storage tank; and miscellaneous monitoring sites in the building and perimeter. There will also be an annunciator panel which will indicate the origin of reactor shutdown (scram) signals.

In operation, the control rods can be actuated by signals from the ion chambers. In addition, signals arising from turbine speed, turbine pressure, and steam bypass will actuate the control rods through the control computer unit. This same unit can transmit signals from the ion chambers to the feedwater temperature control valve.

RE-8-18029-A
H.H.HOOKER:F.S.,4-19-56

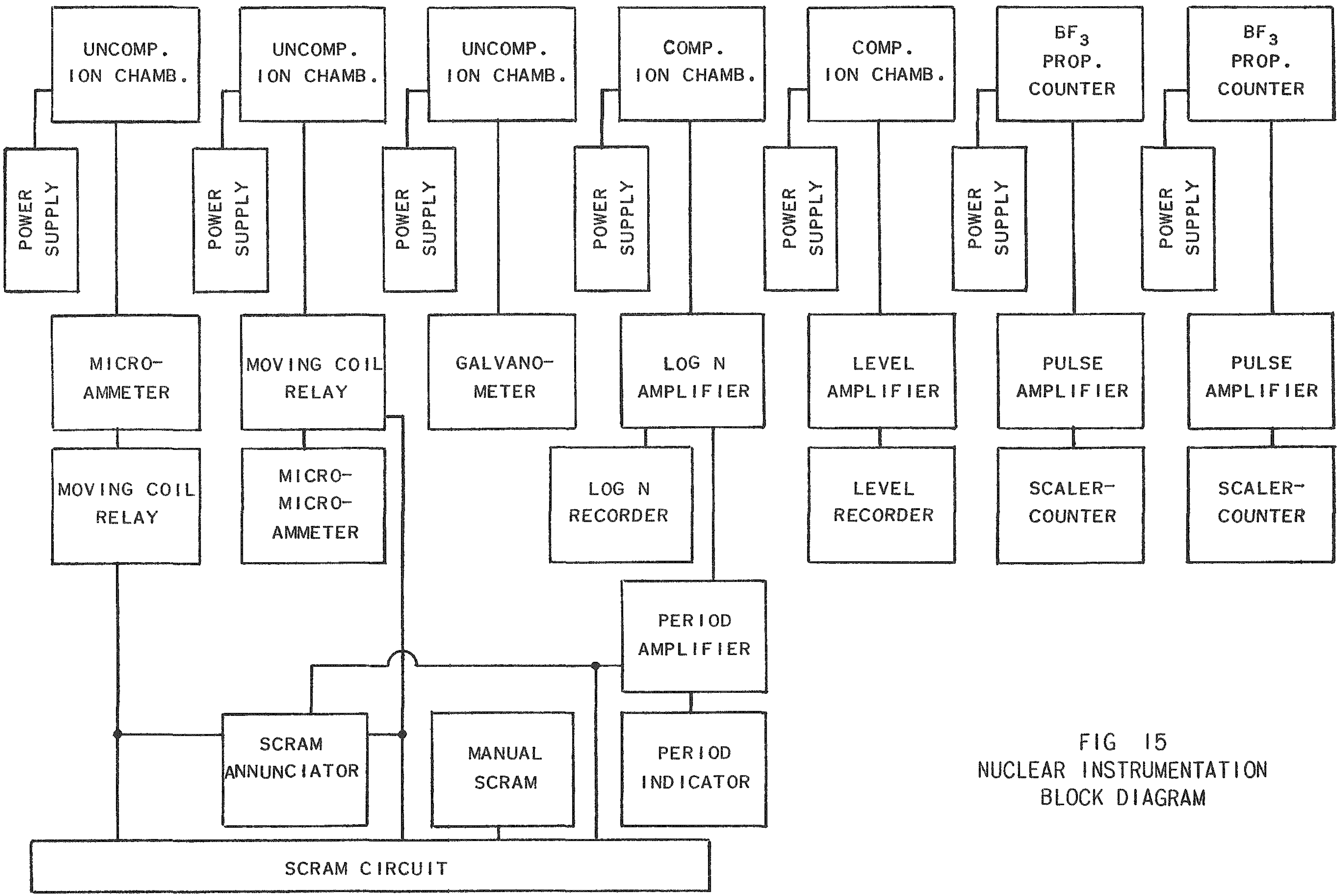

FIG 15
NUCLEAR INSTRUMENTATION
BLOCK DIAGRAM

Table 13

NUCLEAR INSTRUMENTATION COMPONENTS

	Quantity
Reactor Operation Instruments:	
Ionization chambers, boron-lined, uncompensated	3
Ionization chambers, boron-lined, compensated	2
BF_3 ionization chambers (used in proportional range)	2
High voltage power supplies (positive and negative for compensated; and positive for uncompensated)	9
Movable-contact relays (microamp level)	2
Multirange, indicating micro-microammeter	1
Log amplifier	1
Period amplifier	1
Linear amplifier	1
Pulse amplifiers (for BF_3 chambers)	2
Scaler - counters	2
Recorders (1 linear; 1 log N)	2
Period indicator (panel meter)	1
Neutron level indicator (microammeter)	1
Neutron level galvanometer	1
Control rod position indicators	9
Control computer to actuate control rods in response to signals from:	
Steam bypass flow	
Turbine speed	
Turbine steam pressure	
Ion chamber	
Annunciator system (to indicate origin of scram)	1
Radioactivity Indication Instruments:	
Air ejector (indicator)	1
Hotwell (indicator)	1
Contaminated water storage (indicator)	1
Multipoint indicator (for room air and misc. monitoring)	1

For purposes of the present Phase-I study, only brief consideration has been given to compiling conditions which would lead to automatic shutdown of the reactor, or would lead an audible or visible alarm. A preliminary list of automatic shutdown conditions may include:

- reactor power beyond preset level;
- reactor period (useful during start-up, only);
- turbine pressure beyond preset limits;
- excess radiation level at air ejector (indicative of a ruptured fuel element);
- excess radiation level at any area monitoring station (indicative of a major break such as a pipe failure);
- failure of ion-chamber power supplies (reactor power-indicating channels, only);
- failure or interruption of electric power to reactor equipment.

VIII. REACTOR PHYSICS

A. Introduction

Since the issuance of ANL-5452[10] two important alterations in specifications have appeared. The change in peak net electrical load from 125 kw to 260 kw (including overload) and the decision to design for a three-year cycle have necessitated an increased reactor core size as well as a larger initial fuel loading. In order to maintain the reactivity implicit to the steam void in the core within levels of earlier stable BORAX operational experience, the core volume has been augmented fifty per cent, and the (cold) metal-to-water ratio has been reduced slightly. (Guide structure and channels for control rods and fuel assemblies contribute significantly to the net core volume.)

The second "alteration" in specifications is not so much a change as it is a detailing of the earlier specification for demand control. Both changes have markedly affected reactor size, fuel loading, and the control method. These effects will be discussed in the appropriate components of this section.

B. Mathematical Model

The use of the two-group diffusion theory and of an homogenized core medium in the earlier study has been continued in the Phase-I analysis. For calculations of control rod worth, one-group diffusion theory was applied where deemed suitable. One-group spherical harmonics (P_3) computations substantially confirmed the applicability of the diffusion theory in the latter case; the P_3 method was used to analyze neutron flux peaking in the water channels separating fuel plates as well. It is expected that a more detailed neutron slowing-down model will be investigated in the Phase-II work.

Fortunately, experimental results for fuel loadings and for determinations of power versus reactivity in the BORAX reactors are available. In Phase II, a program of comparison study of ALPR and BORAX will be carried on in an effort to minimize the inaccuracies of ALPR calculations.

C. Reactivity Changes During Operation; Effect on Initial Loading of Fuel (U^{235}) and of Burnable Poison (B^{10})

The initial loading of U^{235} has been calculated, in terms of two-group diffusion theory, to be of the order of 13 kg to 14 kg, divided among forty fuel assemblies. The fresh reactor will contain 20 grams to 30 grams of B^{10}. A slight variation in the basic number of fuel assemblies in the core does not have a marked effect on this mass. It is rather the detailed structure of the assembly (especially the metal-to-water ratio) and of the control channels that determines the loading. Studies of the relative merits of reducing the metal content of these channels are continuing. Although neutron flux peaking there is considerably enhanced (with control rods out) when a larger volume fraction is alloted to water, the over-all neutron leakage from the core is reduced, and a net reduction in the fuel requirement is possible. On the other hand, the worth of the control rods is then adversely affected, and this may eventually militate against such an increase in water volume.

As shown in the Phase-I drawings, space has been provided for a total of sixty fuel assemblies. The extra locations will be utilized if the reactor operation at power should not be so steady as desired, if the theoretical analysis has resulted in a demonstrable underestimation of the initial fuel loading, or if the effects of non-uniform burnup should prove to be more severe than predicted theoretically. Insertion of such additional assemblies would, of course, increase the total fuel mass. It has been calculated that the addition of twenty assemblies and associated control channel leads to a 4% reactivity gain.

Included in the estimate of fuel requirement is a total of 4.3 kg earmarked for the maximum total energy, 9 mwy, anticipated for three years of operation. Actually only 0.7 kg of fuel would be saved in three years if the reactor power could be adjusted to conform perfectly with the load. It is suggested that this 0.7 kg be added to the prototype reactor as a cushion against the uncertainty of predicted versus actual thermal efficiency, and such other uncertainties as the useful fraction of the assumed 200 mev per fission and the energy requirements of unused bypassed steam.

Reactivity losses during operation arise from neutron absorption by monotonically increasing concentrations of xenon-135 and other fission products, from the incomplete burnup of the burnable poison (B^{10}), and from the non-uniform burnup of fuel in the core. The average thermal neutron flux in the fuel is 8×10^{12} neutron cm/(cm^3)(sec) in the fresh reactor; it rises to 1.2×10^{13} in the fully depleted reactor. Consequently the "equilibrium" xenon concentration (at full power) rises slightly as the fuel is consumed. Of greater importance, however, is the accompanying problem of overriding the increasing maximum effective xenon concentration reached after a fast complete shutdown from a 3-mw equilibrium level. If sufficient B^{10} is added to the reactor to assure criticality at the beginning and end of the operating cycle, with control rods withdrawn, a net gain in reactivity results from the interaction of fuel and of B^{10} burnup. However, toward the end of the cycle there may be insufficient reactivity available for full power override of maximum xenon, attained five to seven hours after complete shutdown. In Phase II, additional studies will be made of the xenon override problem, and one of several alternatives will be selected, e.g.:

1. add reactivity in the form of extra fuel,

2. wait for an anticipated maximum of perhaps thirteen hours after shutdown, until the equilibrium concentration level is regained,

3. override xenon at reduced power, if necessary.

The buildup of fission product absorption (other than that of xenon-135 and samarium-149) was assumed to be directly proportional to the integrated fission rate, and, as in the earlier study, a microscopic neutron absorption cross section of 80 barns was assumed. An attempt will be made, in Phase II, to arrive at a less pessimistic, more realistic estimate of this cross section. As has been observed (e.g., by J. B. Sampson of KAPL[13]), there is considerable uncertainty with regard to an appropriate cross section, but 80 barns is, very likely, an overestimate. The fission product absorption is then worth almost 6% in reactivity at full depletion, equivalent to approximately 1 kg of U^{235} in the depleted reactor.

Of course, not all of the time dependent effects on reactivity are negative. For example, neutron flux peaking in the water channels separating fuel plates and in the control channels is reduced with operation. As the fuel and B^{10} are consumed, the absorption cross section of the fuel plate drops, reducing the degree of heterogeneity of the assembly absorption and, consequently, the flux peaking in the water. The same argument applies to the larger "sandwiches" of control channels and fuel assemblies. Since the water is a parasitic absorber, the reduction in relative flux leads to reactivity gain.

The increase in the thermal diffusion area results in greater thermal neutron leakage from the reactor; however, this is a smaller effect than the reduction in parasitic neutron absorption. Even this loss in reactivity is accompanied by an advantage, for more thermal neutrons now reach the control rods and the rod worth is enhanced.

D. Reactor Control

1. Feasibility of Reflector Control in the Present ALPR

In the introduction to this chapter, allusion was made to the effects on reactor core size, etc., of increasing the peak net electrical load to 260 kw and the total reactor energy output almost to 9 mwy from the more modest requirements of the earlier design. The core size was augmented fifty per cent to keep the steam void reactivity small. In section D-2, the peak net reactivity gain during operation will be discussed. It is more difficult to flatten the reactivity variation with burnup when a larger fraction of the initial fuel loading is consumed during operation, as is now the case. In the three year reactor operating at the lower power level, the peak net reactivity gain was determined to be approximately 2.5 to 3%, as compared with the estimate of twice this number for the present design.

In the earlier design several reflector control methods were considered in view of the small core volume and of the small control requirements. A match of control needs and control availability was then possible. For the larger reactor this control match is much more difficult if not impossible to achieve by reflector control. For the forty-assembly reactor, the removal of the entire radial reflector reduces reactivity by 6% (using a 3-cm extrapolation distance for the neutron flux in the radial direction). Thus, a combination of reflector control, to adjust reactor heat output to the load, and an additional shim control of long term reactivity changes would be required.

Added to the complication of magnitude of control is the stipulation of a rapid adjustment of reactor power to load. Both requirements can be satisfied by the use of absorbing rods; solid control rods, positioned by mechanical or magnetic drives, have been chosen because their technology is more advanced at this time.

2. Control Rods

It may seem strange that the reactivity loss engendered by fuel burnup was not discussed earlier in the section concerned with such losses. Of course, it is a reactivity loss, when considered from the base point of the fresh reactor. From the standpoint of the depleted reactor, the addition of fuel for burnup is a positive reactivity contribution, and it must be counteracted somehow. The method considered to date is the dispersion of boron (B^{10}) in the fuel meat; the net effect of the relative burnup of fuel and boron is positive. As described in considerable detail in the earlier report,[10] the resulting net reactivity rises to a maximum at approximately mid-cycle and then falls. The reactivity vs time curve is essentially symmetric with respect to mid-cycle, at least as computed to date and even when a considerable degree of burnup nonuniformity is assumed. The peak reactivity gain is approximately 5%, as computed on the basis of uniform burnup. The thermal neutron flux is distorted, however, both by the non-uniform distribution of steam void and by the partial insertion of control rods required to balance the reactivity gain with initial operation. These distortions are similar - the flux peaks below the vertical center of the core. It is believed that the actual non-uniform burnup will lead to a somewhat larger maximum reactivity gain than the 5% predicted by uniform burnup analysis.

The major reactivity gains would occur if it should be necessary to shut down the reactor and to allow the fluid in the reactor to cool to room temperature. The reactivity gain in going from the condition of full power operation to the condition of the reactor at room temperature, and without xenon or samarium, is approximately 10%, roughly allocated as follows:

a. $\frac{\Delta k}{k}$ (loss of xenon and samarium) = + 0.025 ,

b. $\frac{\Delta k}{k}$ (loss of steam void) = + 0.020 to 0.025 ,

with the remainder arising from the negative temperature coefficient of reactivity (including density effects).

This situation is extreme, perhaps, for the decay of xenon and samarium is rather slow, and there is much residual heat in the fuel elements. However, it is desirable to be able to control the worst situation with the control rods available.

As mentioned in the preceding section, the addition of twenty assemblies contributes 4% in reactivity.

The correctly summed reactivity distribution yields the result that it would be desirable to provide approximately 20% in control for the worst situation presently perceivable.

In the Phase I reference design there are five cross control rods, each with a fourteen-inch span. The analysis completed to date indicates that these five rods provide adequate control for the initial operating period of the forty-assembly reactor, and, indeed, for the lifetime of that reactor.

Since the rod worth increases as the fuel is consumed, perhaps these five rods will be sufficient to handle even some of the extra fuel assemblies. As a precautionary measure, four locations are available for special T-shaped absorbing rods. In the actual fresh reactor, the worth of the five cross rods can be determined in time to order additional rods should this be considered advisable.

E. Reactivity in Steam Void

The mean steam void in the fuel assembly fluid has been estimated(14) to be 11.5% on the basis of recent boiling heat transfer data. The reactivity in steam is determined, to a considerable degree, by the detailed guide structure for the control rods, specifically by its metal-to-water ratio. To keep $\Delta k/k$ in steam small, it is desirable to minimize the metal content of the structure. An undesirable aspect of such minimization is the resulting maximization of thermal neutron flux peaking in the control channels when the rods are withdrawn. As a result, the control channels absorb more neutrons and, in fact, they act as rather effective control rods themselves. When the rods are inserted, flux peaking in the channels is reduced, and the neutron absorption in the rods must be increased to maintain their effectiveness. It appears to be a losing battle for the rods, i.e. the net rod effectiveness decreases as the water content in the control channels is increased. A more detailed investigation of the optimum channel structure will be carried out in Phase II.

For this reason, the reactivity in steam has been listed (section D-2) as 2 to 2.5%, the former value applying to the channel with a cold metal-to-water ratio of approximately unity.

A corollary of peaking in control is the neutron flux peaking in the parts of the fuel assemblies adjacent to the control channels. The hot spots created should not prove to be troublesome, in view of the low average heat flux in this reactor.

F. Appendix to the Physics Section

Introduction

In the earlier report,(13) fundamentals of the physics analysis were discussed at length and a detailed tabulation of results was presented. In this report, therefore, emphasis has been placed on the important differences, largely arising from alterations in specifications, between the earlier design and the Phase-I reference reactor design. It was decided to present the important new numerical results in the text rather than repeat much of the previous report. With this concept in mind, the author of this section has attempted a rather free-wheeling discussion of the Phase-I physics, indicating present uncertainties and the direction of the Phase-II effort. Much of the detailed analysis has been presented in the form of Argonne internal memos.

The purpose of this appendix is to discuss briefly those aspects of the Phase-I physics analysis which differ from the methods used in the earlier report.

Flux Peaking in Channels

The disadvantage factor of the fuel plates in the lattice of fuel and water channel was calculated with the aid of a (P_3/spherical harmonics) routine on the AVIDAC. The effects of temperature, of the fluid density in the channels, and of fuel burnup were investigated and the results interpreted as a suitable homogenization of the core medium. Such local flux peaking as occurs at the central web of the fuel assembly and between fuel assemblies was estimated; these results were incorporated in the general disadvantage factor.

Thermal neutron flux peaking in the control channels was calculated by one-group diffusion theory with a step-function source of thermal neutrons, the magnitude of the step being the ratio of the effective water volume fraction in the control channel to that in the fuel assemblies. Since the fuel does not extend to the edge of the assembly, the effective control channel is at least 1.34 in. thick. The P_3 routine was applied to these problems, as well; the diffusion theory solution in the assembly region was confirmed, but the P_3 method yielded a slightly greater flux rise in the control channel.

Effective Neutron Temperature

In the earlier report, it was assumed that the effective neutron temperature (kT) corresponds to the temperature of the bulk fluid. A correction factor was then applied to obtain the greater fuel mass required if the neutron kT should be larger. In the Phase-I analysis, an attempt was made to include the effects of absorption and scattering in hardening the thermal neutron flux spectrum (in terms of an effective shift in the mode, kT, of a Maxwellian distribution of thermal flux).

Since the basic work of Wigner and Wilkens,[15] several reports have appeared in which elaborations on this method have been described. The efforts of Avery and Krasner,[16] (ANL), Brown and St. John[17] (du Pont), of Zweifel and Petrie[18] (KAPL), and especially of Coveyou, Bate, and Osborne[20] (ORNL) may be mentioned. A compromise solution was adopted for ALPR analysis, using the formulas of reference 19 together with the notion of an effective mass of 2 (reference 17) for the calculation of energy exchange between neutrons and water molecules in the thermal energy range.

Neutron Cross Sections and Other Parameters

Except for:

$$\eta\, U^{235} = 2.08$$

$$\sigma_a^{U^{235}}\ (0.0253) = 687\text{b}$$

$$(1 + \alpha)(U^{235}) = 1.184$$

the basic cross sections used in the earlier report[10] were used.

IX. REACTOR COST ESTIMATE

	Unit Cost	Number Required	Total Cost
Core structure	$6,400	1	$6,400
Fuel element assembly	850	52	44,200
"Dummy" fuel element assembly	100	16	1,600
Control Rod	1,137	6	6,822
Mechanical Rod Drive	10,000	6	60,000
Fuel Element Coffin	5,370	1	5,370
Nuclear Instrumentation	40,000	1	40,000
Periscope	1,000	1	1,000
Manipulator	1,000	1	1,000
Subtotal			$166,392
Installation, 25%			41,598
Subtotal			207,990
Contingencies, 10%			20,799
Grand Total			$228,789

REFERENCES

1. Humphreys, J. R., "Effects of Reactor Radiation on High Temperature Static Water System," Paper No. 740, International Conference on Peacetime Uses of Atomic Energy, Geneva, Switzerland (Aug. 1955).

2. Rockwell, T. and P. Cohen, "Pressurized Water Reactor (PWR) Water Chemistry," Paper No. 536, International Conference on Peacetime Uses of Atomic Energy, Geneva, Switzerland (Aug. 1955).

3. Gutzeit, G., "Kanigen Nickel Plating," Metal Progress 66, 113 (1953).

4. Draley, J. E. and W. E. Ruther, "Corrosion Resistant Aluminum above 200°C," ANL-5430 (July 15, 1955).

5. Private Communication from H. Pearlman.

6. Private Communication from N. R. Grant.

7. Private Communication from N. R. Grant.

8. Ref. 4, p. 29.

9. Unpublished data, personally communicated by G. A. Reed.

10. "Design Study of a Nuclear Power Plant, etc.," Treshow, M., A. R. Snider and D. H. Shaftman, ANL-5452 (May, 1955).

11. Chemical Engineering Division Summary Report, October, November, December 1955, ANL-5529 (February 10, 1956).

12. Unpublished data, personally communicated by C. B. Zitek and V. C. Hall, Jr.

13. J. B. Sampson, et al., "Poisoning in Thermal Reactors Due to Stable Fission Products," KAPL-1226 (October 4, 1954).

14. Private Communication from Professor A. L. London, Stanford University.

15. E. P. Wigner, J. E. Wilkins, Jr., "Effect of the Temperature of the Moderator on the Velocity Distribution of Neutrons with Numerical Calculations for H as Moderator," AECD-2275 (September 14, 1944).

16. R. Avery, S. Krasner, "Energy Distribution of Thermal Neutrons in a Water Moderator," Naval Reactor Program Quarterly Reports, ANL-4842 (June 15, 1952) p. 22; ANL-4898 (September 15, 1952) p. 13.

17. H. D. Brown, D. S. St. John, "Neutron Energy Spectrum in D_2O," DP-33, (February 1954).

18. P. F. Zweifel, C. D. Petrie, "Averages of Thermal Cross Sections for Hydrogen-Moderated Assemblies," KAPL-1469 (January 1, 1956).

19. R. R. Coveyou, et al., "Effect of Moderator Temperature Upon Neutron Flux in Infinite, Capturing Medium," ORNL-1958 (October 20, 1955).

ACKNOWLEDGEMENT

The cooperation of members of the Remote Control Division and of the Metallurgy Division of Argonne National Laboratory is gratefully acknowledged.

The ALPR is primarily a project of the Reactor Engineering Division and many members of the Division have made significant contributions to the Phase-I design study.

The Drafting Section and Secretarial Section of the Reactor Engineering Division have been particularly helpful in their interested efforts in expediting the work.